© 2022. Published by The Company of Biologists Ltd | Journal of Cell Science (2022) 135, jcs259789. doi:10.1242/jcs.259789

RESEARCH ARTICLE

A transcriptionally repressed quiescence program is associated with paused RNA polymerase II and is poised for cell cycle re-entry

Hardik P. Gala[1,2,*], Debarya Saha[1,*], Nisha Venugopal[1,2], Ajoy Aloysius[1,2,3], Gunjan Purohit[1] and Jyotsna Dhawan[1,2,‡]

ABSTRACT

Adult stem cells persist in mammalian tissues by entering a state of reversible quiescence, referred to as G_0, which is associated with low levels of transcription. Using cultured myoblasts and muscle stem cells, we report that in G_0, global RNA content and synthesis are substantially repressed, correlating with decreased RNA polymerase II (RNAPII) expression and activation. Integrating RNAPII occupancy and transcriptome profiling, we identify repressed networks and a role for promoter-proximal RNAPII pausing in G_0. Strikingly, RNAPII shows enhanced pausing in G_0 on repressed genes encoding regulators of RNA biogenesis (such as *Ncl*, *Rps24*, *Ctdp1*), and release of pausing is associated with increased expression of these genes in G_1. Knockdown of these transcripts in proliferating cells leads to induction of G_0 markers, confirming the importance of their repression in establishment of G_0. A targeted screen of RNAPII regulators revealed that knockdown of Aff4 (a positive regulator of elongation) unexpectedly enhances expression of G_0-stalled genes and hastens S phase; however, the negative elongation factor (NELF) complex, a regulator of pausing, appears to be dispensable. We propose that RNAPII pausing contributes to transcriptional control of a subset of G_0-repressed genes to maintain quiescence and impacts the timing of the G_0-G_1 transition.

This article has an associated First Person interview with the first authors of the paper.

KEY WORDS: Quiescence, Myoblast, Adult stem cells, Promoter-proximal RNA polymerase pausing, Cell cycle re-entry, NELF, Aff4

INTRODUCTION

In mammalian tissues, adult stem cells exist in a state of reversible arrest or quiescence. This 'out of cycle', or G_0, phase is characterized by the absence of DNA synthesis; highly condensed chromatin; and reduced transcriptional, translational and metabolic activity. In contrast to their terminally differentiated counterparts, quiescent cells retain the ability to re-enter the cell cycle, which is crucial for stem cell functions such as self-renewal and regeneration. Entry into G_0 involves not only the induction of a specific quiescence program (Coller et al., 2006; Fukada et al., 2007; Liu et al., 2013; Subramaniam et al., 2013) but also suppression of alternate arrest programs such as differentiation, senescence and death (Sousa-Victor et al., 2014; Cheedipudi et al., 2015; García-Prat et al., 2016).

Several lines of evidence suggest that quiescent cells are held in readiness for cell cycle re-entry by mechanisms that keep the genome poised for activation. For example, when cells enter G_0, there is an increase in epigenetic modifications (trimethylation of histone H4 on lysine 20) that promote the formation of facultative heterochromatin and chromatin condensation, and trigger transcriptional repression (Boonsanay et al., 2016; Evertts et al., 2013), while other histone modifications help to maintain the quiescence program (Srivastava et al., 2010; Juan et al., 2011; Mousavi et al., 2012; Liu et al., 2013; Woodhouse et al., 2013). Chromatin regulators induced specifically in G_0 hold genes encoding key cell cycle regulators in a poised state (Cheedipudi et al., 2015) by preventing silencing. Importantly, epigenetic regulation in G_0 ensures that the repression of lineage determinants such as MyoD (also known as MyoD1) is reversible, helping to preserve lineage memory (Sebastian et al., 2009). The quiescence program also necessitates mechanisms that balance the global repression of transcription with a readiness for rapid reversal. G_1 cells exhibit markedly higher RNA levels than cells in G_0 (Darzynkiewicz et al., 1980), but mechanisms that control this rapid and widespread transcriptional induction are not completely understood.

Early studies on reversible quiescence in fibroblasts revealed a rapid loss of RNA synthesis upon entry into G_0. The rapid restoration of global protein synthesis during exit from G_0 into G_1 preceded RNA synthesis, leading to the conclusion that transcripts essential for cell cycle re-entry are stored in G_0 (Benecke et al., 1978; Roy et al., 2021). However, subsequent studies have led to the discovery of immediate early genes (IEGs; such as *Fos*, which encodes c-Fos) whose expression is transcriptionally induced within minutes of activation and does not require new protein synthesis (Lau and Nathans, 1985; Iyer et al., 1999). Despite extensive analysis of transcriptomic changes accompanying the G_0-G_1 transition (Coller et al., 2006; Sajiki et al., 2009; Cheung and Rando, 2013), a comprehensive understanding of the transcriptional machinery during quiescence is lacking.

The regulation of RNA polymerase II (RNAPII) is an integral part of the transcription cycle, with cell type- and cell state-specific control (reviewed in Adelman and Lis, 2012; Puri et al., 2015). In quiescent adult stem cells, RNAPII itself exhibits reduced activation (Freter et al., 2010), whereas Mediator complex subunit 1 (MED1) is associated with maintenance of quiescence (Nakajima et al., 2013), and transcription factor complex II (TFII) proteins have been implicated in differentiation (Deato and Tjian, 2007; Malecova et al., 2016). In yeast, RNAPII activity is under direct control of cyclin–cyclin-dependent kinase (CDK) complexes contributing to

[1]Centre for Cellular and Molecular Biology, Hyderabad 500007, India. [2]Institute for Stem Cell Science and Regenerative Medicine, Bangalore 560065, India. [3]National Center for Biological Sciences, Bangalore 560065, India.
*These authors contributed equally to this work

‡Author for correspondence (jdhawan@ccmb.res.in)

H.P.G., 0000-0001-8418-9346; D.S., 0000-0002-3919-0978; N.V., 0000-0002-8172-1138; A.A., 0000-0001-6705-4810; G.P., 0000-0002-6737-0968; J.D., 0000-0001-7117-7418

Handling Editor: John Heath
Received 20 January 2022; Accepted 27 June 2022

Journal of Cell Science (2022) 135, jcs259789. doi:10.1242/jcs.259789

cell cycle-dependent transcriptional state (Kõivomägi et al., 2021). However, while components of the RNAPII complex contribute to cell state changes, global RNAPII regulation in reversible quiescence is poorly explored. It is now well established that rather than regulation of transcription initiation, elongation control at the level of promoter-proximal RNAPII pausing regulates starvation-induced stationary phase in yeast; developmental programs in flies; and stress-induced genes, neuronal IEGs and mitogen-induced genes in mammalian cells (Saha et al., 2011; Levine, 2011; Gaertner et al., 2012; Adelman and Lis, 2012; Radonjic et al., 2005). During early elongation, RNAPII pauses 20–60 bp downstream of the transcription start site (TSS) due to the presence of negative elongation factors [including the negative elongation factor (NELF) complex and DRB sensitivity-inducing factor (DSIF) complex]. This pause is signal responsive and is released upon signal-dependent recruitment of positive transcription elongation factor b (P-TEFb) by the super elongation complex (SEC). SEC, a multi-protein complex with kinase activity, assembles around scaffold proteins of the AF4 family (Aff1 or Aff4) and has been shown to be essential for signal-dependent activation of transcription via release of paused RNAPII. RNAPII pausing allows genes to be poised for future expression (Kouzine et al., 2013) and appears to mark regulatory nodes prior to a change in developmental state, allowing coordinated changes in gene networks. We hypothesized that withdrawal of cells into reversible arrest might be associated with a distinct anticipatory program marking a specific set of paused genes that may play a critical role in subsequent cell transitions.

Arrest and activation of muscle stem cells (MuSCs) are critical for adult muscle repair and regeneration (Pallafacchina et al., 2010; Rodgers et al., 2014; Machado et al., 2017). We have previously used a culture model employing C2C12 mouse myoblasts to recapitulate the reversibly arrested stem cell state (Milasincic et al., 1996; Sachidanandan et al., 2002; Yoshida et al., 1998), enabling genome-wide analysis of G_0, as distinct from early G_1 (Sebastian et al., 2009; Subramaniam et al., 2013; Cheedipudi et al., 2015). Notably, genes identified as induced in cultured G_0 myoblasts mark MuSCs *in vivo* (Sachidanandan et al., 2002; Doles and Olwin, 2015), strengthening the utility of this model. Here, we investigated global quiescence-associated transcriptional repression in reversibly arrested myoblasts. Using ChIP-seq and RNA-seq, we elucidated RNAPII occupancy and the extent of transcriptional repression during reversible cell cycle arrest, thereby identifying poised transcriptional networks characteristic of G_0. We used knockdown analysis of G_0-specific stalled genes, as well as known regulators of RNAPII activity, to delineate the role of pausing in quiescence-associated functions. Our results suggest a model wherein promoter-proximal RNAPII pausing may preconfigure specific gene networks whose repression aids entry into and maintenance of G_0. We also uncovered a surprising restrictive role for the SEC regulator Aff4 in transcriptional activation of poised networks, which appears to confer appropriate timing to the G_0-G_1 transition.

RESULTS

Quiescent cells display reduced RNA content, low RNA synthesis, low RNAPII processivity and cytoplasmically localized RNAPII

Global transcription mediated by all three RNA polymerases is dynamic across the cell cycle (White et al., 1995; Yonaha et al., 1995; Russell and Zomerdijk, 2005) and is dampened during cell cycle exit (Hannan et al., 2000; Scott et al., 2001; Russell and Zomerdijk, 2005). Using flow cytometry, we found that the decrease in total cellular RNA content is evident in reversibly arrested myoblasts (G_0) compared to that of proliferating myoblasts (referred to hereafter as MBs) (Fig. 1A). To determine whether this suppression is common to cells entering alternate states of arrest, we used quantitative *in situ* imaging, because differentiated myotubes (MTs) are syncytia that cannot be reliably analyzed using flow cytometry. We observed that the total RNA content per cell in reversibly arrested G_0 cells was markedly lower than that of either MBs or terminally arrested MTs (Fig. 1B; Fig. S1A). Furthermore, a time course of quiescence reversal showed that a rapid and robust increase in RNA content occurred within 30 min of cell cycle re-entry and was sustained as cells entered S phase (Fig. 1B; Fig. S1B). To assess the contribution of RNA synthesis to the reduced steady-state levels of RNA in G_0 cells, we used pulse-labeling with 5-ethynyl uridine (EU) (Jao and Salic, 2008) (Fig. 1C; Fig. S1C). EU incorporation into newly synthesized RNA was strongly suppressed in G_0 cells compared to that of MBs and sharply increased within 30 min of activation, correlating with the rise in RNA content (Fig. 1B,C), which indicates a very rapid restoration of the transcriptional machinery upon cell cycle re-entry.

To evaluate the transcriptional output of MuSCs in their niche, we isolated single myofibers with associated satellite cells and determined their EU incorporation. We found that reversibly arrested MuSCs *ex vivo* also show robust RNA synthesis within 3 h of isolation, whereas differentiated myofiber nuclei in the same sample showed low incorporation of EU (Fig. 1D; Fig. S1D). This observation is consistent with evidence that MuSCs on freshly isolated fibers have already exited from quiescence during the process of myofiber isolation (Fukada et al., 2007; Zhang and Anderson, 2014; Machado et al., 2017; van Velthoven et al., 2017; Yue et al., 2020).

To gain insights into the status of RNAPII, we assayed levels of RPB1 (also known as POLR2A), the largest subunit of RNAPII, and its phosphorylated forms that mark distinct stages of the transcription cycle – initiation (phosphorylation of serine 5 of the C-terminal repeat domain sequence, Ser5-p) and elongation (phosphorylation of serine 2 of the C-terminal repeat domain sequence, Ser2-p) (Zhang et al., 2012). Total RNAPII showed decreased abundance in both G_0 cells and MTs compared to the abundance in MBs (Fig. 1E,F; Fig. S1E–G), as assayed using both western blotting and immunostaining. Furthermore, quantitative imaging revealed that while both G_0 cells and MTs showed decreased nuclear levels of RNAPII compared to the levels in MBs (Fig. 1F; Fig. S1E for quantification), RNAPII in G_0 cells was largely localized in the cytoplasm.

Taken together, the comparison of steady-state RNA levels and active RNA synthesis per cell shows that global reduction in RNA content distinguishes quiescence from both proliferation and differentiation. This G_0-specific reduction of global RNA levels results directly from depressed RNA synthesis, which is rapidly reversed in a transcriptional burst within minutes of cell cycle reactivation. Furthermore, since total RNA levels are maintained in irreversibly arrested MTs, strong global repression of RNA biogenesis is not a general function of cell cycle cessation but rather is characteristic of a specific quiescence program.

Identification of a quiescence-specific RNAPII-mediated regulatory program

Transcriptome analysis of quiescent myoblasts using RNA-seq

Previous studies have identified quiescence-regulated genes in variety of cell types, including myoblasts (Venezia et al., 2004; Coller et al., 2006; Subramaniam et al., 2013) and MuSCs

Journal of Cell Science (2022) 135, jcs259789. doi:10.1242/jcs.259789

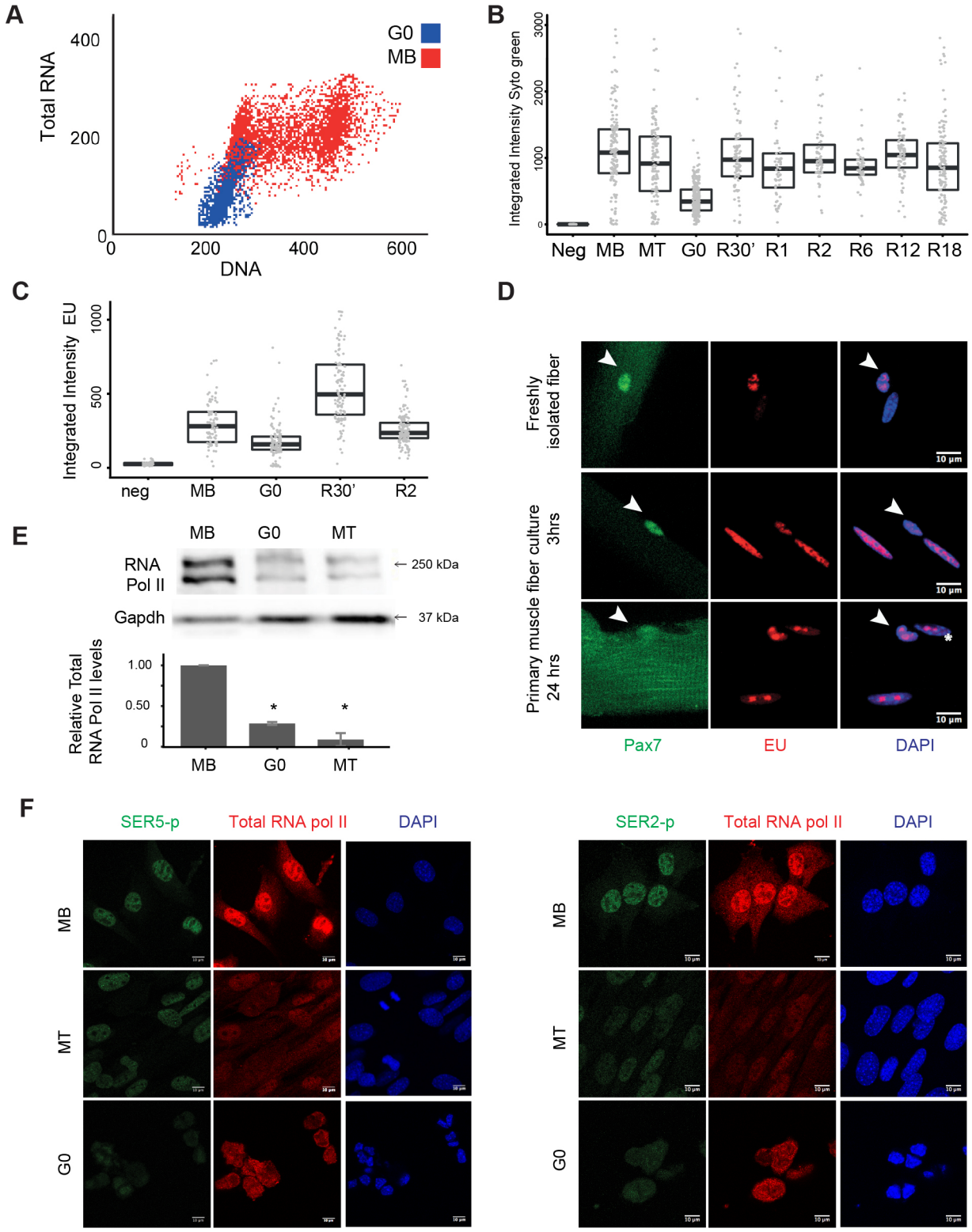

Fig. 1. See next page for legend.

(Fukada et al., 2007; Pallafacchina et al., 2010; Liu et al., 2013; van Velthoven et al., 2017; Machado et al., 2017). However, all these studies employed equivalent RNA as means of normalization, which strongly affects the number of differentially expressed genes that can be confidently identified (Lovén et al., 2012), particularly when cellular RNA content varies sharply across the compared samples (as documented in Fig. 1A,B). To overcome this issue, we quantitatively re-investigated the transcriptome of quiescent myoblasts using RNA-seq analysis, where gene expression was measured by normalization to equal cell number and not equal RNA (described in Materials and Methods; Fig. S2A,C; Srivastava et al., 2018). Furthermore, an unbiased

Journal of Cell Science (2022) 135, jcs259789. doi:10.1242/jcs.259789

Fig. 1. Decreased total RNA content, repressed total RNA synthesis, and downregulation of RNAPII abundance and activation in quiescent myoblasts and satellite cells. (A) Flow cytometric quantification of total RNA (SYTO Green staining intensity; arbitrary units) versus DNA content (DRAQ5 staining intensity; arbitrary units) shows reduced RNA content in G_0 cells (blue) compared to MBs (red). Dot plots show ∼50% reduction in total RNA in G_0 cells compared to the G_1 population of MBs. *n*=3. Data shown are representative plot generated from one experiment. (B) Total RNA content in distinct cell states revealed by fluorescence imaging of MBs, G_0 cells and MTs stained using SYTO Green; nuclei were counterstained with DAPI (see images in Fig. S1A). CellProfiler was used to quantitate integrated image intensity values per cell (arbitrary units) for the three cell states as well as across a time course of reactivation from G_0 from 30 min to 18 h (R30′ to R18). Neg, unstained MB cells. *n*>120 cells for MB, MT and G_0; *n*>60 cells for reactivation time points. G_0 compared to all other time points, $P<2\times10^{-16}$; between MB and MT, $P=0.072$ (Mann–Whitney test). (C) Newly synthesized RNA revealed by EU incorporation in a 30 min pulse. Quantification of EU incorporation (integrated intensity EU, arbitrary units) was performed by image analysis, as described in B (see images in Fig. S1C), for MBs, G_0 cells, and cells reactivated from G_0 for 30 min (R30′) or 2 h (R2), as well as a negative control sample (neg, MB cells without EU pulse). *n*>80 cells. Significant differences were observed for comparisons between G_0 and MBs, R30′ or R2 ($P<2\times10^{-10}$); and between MBs and R30′ ($P=2\times10^{-14}$); however, comparison between MBs and R2 showed no significant difference (Mann–Whitney test). Boxplots in B and C show median values (horizontal bars) and the 25th to 75th percentile (boxes). (D) Active RNA synthesis in MuSCs associated with single myofibers cultured *ex vivo*. MuSCs (arrowheads), which are marked by Pax7 (green), can be distinguished from differentiated myonuclei (MN; asterisk), which are Pax7 negative, within the underlying myofiber. In freshly isolated fibers, EU exposure (red) during a 30 min pulse *ex vivo* leads to EU incorporation only in MuSCs and not in MN, indicating rapid activation of RNA synthesis in MuSCs during the isolation protocol. At 3 h and 24 h post isolation, MN also show RNA synthesis (observed as EU incorporation) at similar levels as MuSCs (quantification is shown in Fig. S1D). Images are representative of 7–9 muscle fibres isolated from two mice. (E) Western blot analysis using antibodies against RNAPII large subunit (total) shows two distinct bands (∼250 kDa) corresponding to hyperphosphorylated and hypophosphorylated RNAPII isoforms. Both cell cycle-arrested states (G_0 and MTs) show reduced levels of RNAPII. GAPDH was used as loading control. The graph shows quantification of relative total RNAPII levels, normalized to MB. Data are presented as mean ±s.d. of *n*=2 experiments. **P*<0.05 (two-tailed unpaired *t*-test). (F) Expression and subcellular localization of RNAPII. Representative immunofluorescence images for MBs, G_0 cells and MTs stained for total RNAPII (large subunit RPB1, red) and active RNAPII (left; Ser5-p, green) or total RNAPII (red) and Ser2-p (right, green). Images are representative of *n*>70 cells imaged and quantified for each cell state (quantification is shown in Fig. S1E). Note that G_0 cells show cytoplasmic staining. Scale bars: 10 µm.

principal component analysis comparing our RNA-seq datasets (from G_0 cells and MBs) with previously published RNA-seq datasets of freshly isolated MuSCs from paraformaldehyde (PFA)-perfused mice (fSCs), MuSCs from unperfused mice (uSCs) and activated satellite cells (ASCs) (Yue et al., 2020), revealed a close clustering of G_0 C2C12 cells with fSCs, but not with uSCs and ASCs. This analysis supports the view that induced quiescence in cultured myoblasts captures the quiescent signature of unperturbed MuSCs *in vivo* (Fig. S2B).

Repressed RNA biogenesis pathways distinguish quiescent cells from differentiated cells

We first evaluated and verified the distinct identities of the two mitotically inactive states (G_0 cells and MTs), in contrast to MBs, using overrepresentation analysis of gene ontology (GO) terms assigned to the differentially expressed genes identified in our equal cell number-normalized RNA-seq datasets. In G_0 cells, terms representing response to external stimuli, stress and extracellular matrix organization were found to be overrepresented among the genes that were upregulated, whereas skeletal muscle contraction and ion transport terms were found to be overrepresented among the genes that were upregulated in MTs (Table S7). Expectedly, genes that were downregulated in the mitotically arrested states (either G_0 cells or MTs) were enriched for GO terms related to cell cycle processes, DNA replication and cell proliferation (Table S8). However, unlike in MTs, ontologies related to RNA metabolism were enriched in the set of genes strongly downregulated in G_0 cells, particularly genes encoding basal transcription factors, RNA polymerases and proteins involved in RNA biogenesis (mRNA, tRNA and rRNAs). Given the observed quiescence-specific reduction of both steady-state and active transcription, we hypothesized that in G_0, transcriptional repression is likely mediated by RNAPII repression, either at the level of abundance and/or processivity. Therefore, we focused on transcriptional control mechanisms in G_0 cells.

Identification of stage-specific RNAPII recruitment in myogenic cells

To identify stage-specific programs of gene expression we used RNAPII enrichment profiling, first validating RNAPII ChIP enrichment (using an antibody specific to the large subunit of RNAPII, RPB1) on the G_0-induced gene *Rgs2* (Subramaniam et al., 2013) (Fig. S2D). Our RNA-seq data confirmed *Rgs2* transcriptional induction in the G_0 cells (Table S4, Fig. S2C). Subsequently, we used ChIP-seq (see Materials and Methods) of duplicate samples of MBs and G_0 cells (Fig. S2E). Globally, RNAPII enrichment was observed at the TSS in both MBs and G_0 cells (data not shown), which is consistent with the 'toll booth' model (Adelman and Lis, 2012) wherein initiated RNAPII may pause, representing a checkpoint for transcription and presaging stage-specific regulation of elongation. Importantly, only a small proportion of promoters in G_0 cells (>90th percentile of promoters based on read density score, representing 1517 genes) showed increased occupancy of RNAPII compared to that in MBs and may represent a G_0-specific class of genes, with elevated ongoing RNAPII recruitment (Fig. 2A).

To evaluate the rate of promoter clearance and gain insights into underlying transcriptional regulation (Zeitlinger et al., 2007), we computed and compared the 'stalling index' (SI) for all genes across MB and G_0 cell samples. The SI was calculated as the ratio of RNAPII density at the promoter region to that across the gene body region, where higher SI reflects a lower promoter clearance of RNAPII and indicates a node of regulation (see Materials and Methods and Fig. S3A–C). Interestingly, more than 50% of analyzed genes displayed an SI greater than 1 in either MBs or G_0 cells, confirming that clearance of engaged RNAPII from the promoter is a significant common regulatory mechanism (Fig. S3C, Tables S9 and S10). Overall, 1650 genes were identified as stalled in G_0 cells, and 1488 genes were identified as stalled in MBs, and expectedly, GO analysis showed that metabolic and stress response ontologies were enriched among the stalled genes identified in MBs and G_0 cells (Fig. S4).

G_0-stalled genes are specifically repressed in quiescence

Since promoter-proximal stalling influences the overall transcriptional output from a given locus, the repertoire of genes regulated by this mechanism in a given state would yield insights into global RNAPII-mediated regulation of that cellular state. Our hypothesis was that control of quiescence might include uniquely stalled genes. Therefore, we analyzed the group of 1650 genes identified as stalled in G_0 cells (hereafter referred to as 'G_0-stalled genes'; Table S9). Genes that were strongly stalled in G_0 cells

Journal of Cell Science (2022) 135, jcs259789. doi:10.1242/jcs.259789

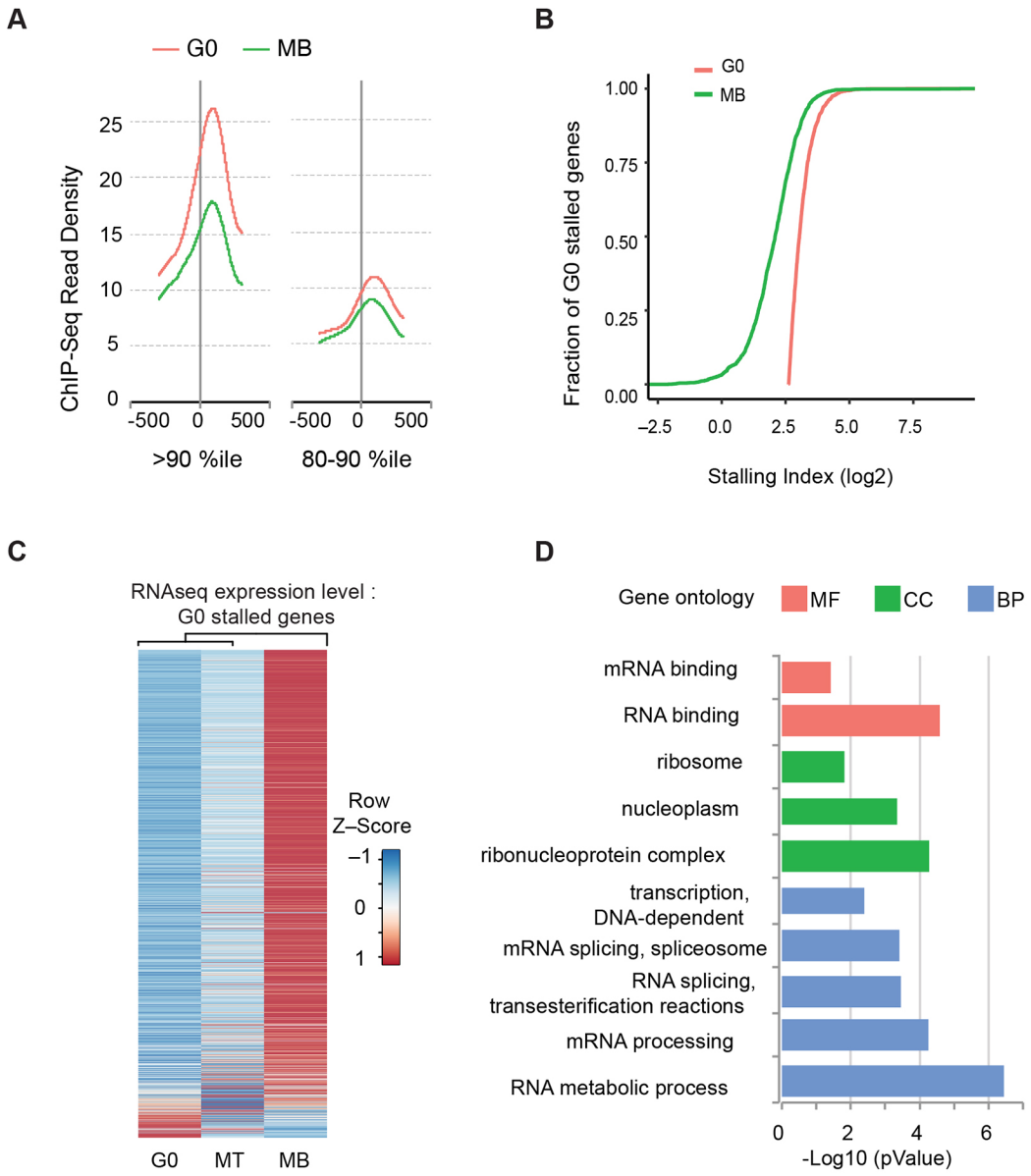

Fig. 2. Quiescence-specific RNAPII-stalled genes are transcriptionally repressed. (A) ChIP-seq analysis of RNAPII indicates a high degree of RNAPII enrichment on a subset of promoters in G_0 cells compared to promoters in MBs. The density of sequencing reads plotted across ±300 bp relative to TSSs is shown. Average RNAPII enrichment densities (plotted as reads per million) are presented for the top two deciles of genes with the highest read density scores [i.e. 1517 genes for each of the 80–90th and >90th percentile (%ile) groups] for each state. Note the substantial difference in peak height around TSSs between G_0 cells and MBs for the >90th percentile gene sets, whereas the peak heights for the 80–90th percentile gene sets are more similar between states. (B) Stalling indices for 1650 genes identified as G_0 stalled (selection criteria as described in the Material and Methods and Fig. S3B) are presented as the cumulative distribution function (CDF) for ChIP samples for the two cellular states. Pairwise comparisons indicates significantly higher SI in G_0 compared to MB (Mann–Whitney test gave $P<2\times10^{-16}$). Data in A and B are based on means of two replicates. (C) Expression analysis of G_0-stalled genes in different cellular states (G_0, MTs, MBs). The heat map represents mRNA expression derived from RNA-seq analysis for genes exhibiting RNAPII stalling specifically in G_0. Less than 2% of these genes are induced (red) in G_0 cells compared the expression level in MBs, whereas ∼60% of G_0-stalled genes are repressed (blue) in quiescence. Data in C are based on means of two replicate RNA sequencing experiments. (D) G_0-stalled genes were analyzed using the PANTHER overrepresentation test, and significantly enriched gene ontologies (BP, biological process; CC, cellular component; MF, molecular function) related to RNA biology with $P<0.05$ [Fisher test with Benjamini–Hochberg FDR (false discovery rate) correction] are shown. Notably, ontologies for RNA binding, ribonucleoprotein complexes and RNA metabolic processes are enriched in the set of G_0-stalled genes.

(high SI) displayed much lower SIs in MBs (Fig. 2B; Fig. S3E, Tables S9 and S11), indicating differential regulation by the stalling mechanism. We found that ∼60% of G_0-stalled genes showed lower expression in G_0 cells compared to their expression in MBs, whereas less than 2% were upregulated in G_0 cells (Fig. 2C; Fig. S3F). Thus, most G_0-stalled and downregulated genes show very low transcriptional activity in G_0 but display high promoter-proximal RNAPII occupancy, indicative of a primed state (Fig. 2B and Fig. S3G). Furthermore, the set of G_0-stalled genes was found to be specifically enriched for GO terms related to mRNA biogenesis and RNA processing, RNAPII-transcribed genes involved in ribosomal machinery, and (nuclear) mitochondria-related genes. We conclude that RNAPII pausing distinguishes specific gene groups in G_0 (Fig. 2D; complete list in Table S12). We compared all genes with

Journal of Cell Science (2022) 135, jcs259789. doi:10.1242/jcs.259789

downregulated expression in G_0 cells to the subset of genes that was both downregulated and stalled in G_0 cells (referred to hereafter as G_0-stalled repressed genes); a specific enrichment of RNA metabolism genes was seen in the G_0-stalled repressed gene subset, while the larger group of genes that were repressed but not stalled contains cell cycle- and muscle-related genes, characteristic of the quiescence program, where both proliferation and differentiation are suppressed (Fig. S3G, GO analysis in Table S13). Thus, a quiescence-associated stalling mechanism appears to selectively target RNA metabolism genes.

G_0-stalled repressed genes are poised for reactivation during G_1

The observations that quiescent cells display reduced RNA levels and that G_0-stalled genes are enriched for regulators of RNA biogenesis and maintenance (Figs 1,2) led us to hypothesize that repressed, stalled genes represent nodes that control RNA metabolism. We therefore analyzed a subset of G_0-stalled repressed genes (*Ncl*, *Ctdp1*, *Rps24*, *Slbp* and *Zc3h12A*) representing RNA metabolism gene ontologies, along with control genes [including genes that were repressed but not stalled in G_0 cells (*Cdk1* and *Cdk6*), *Fos* (an IEG repressed in G_0 cells but rapidly induced during G_0-G_1 transition) and *Rgs2* (a gene with upregulated expression in G_0 cells)] to establish their transcriptional output upon exit from quiescence. We hypothesized that the G_0-stalled genes would undergo a reversal of stalling during G_0-G_1 transition, when RNA biogenesis is a key requirement. The selected genes (detailed below) showed high RNAPII stalling in G_0 (Fig. 2B; Fig. S5A) and displayed activating histone marks (trimethylation of histone H3 on lysine 4) but not repressive marks (trimethylation of histone H3 on lysine 27) (Fig. S5D), which is consistent with a primed state. These selected genes encode nucleolin (Ncl, which controls rRNA biogenesis), ribosomal protein S24 (Rps24, a structural component of ribosomes), RNAPII recycling enzyme C-terminal domain phosphatase (Ctdp1, which regulates RNAPII activity), stem-loop-binding protein (Slbp, which regulates the stability of stem-loop-containing histone mRNA) and zinc finger CCCH-type-containing 12A (Zc3h12A, an RNase that modulates miRNA levels). We used reverse transcription-quantitative PCR (RT-qPCR) to evaluate induction of these genes during cell cycle re-entry. Within the first 30 min of reactivation, all the selected G_0-stalled repressed genes (*Ncl*, *Rps24*, *Ctdp1*, *Zc3h12A* and *Slbp*) exhibited a significant increase in normalized mRNA levels (at 30 min, referenced to G_0; Fig. 3A), similar to the known kinetics of the IEG *Fos* (Kami et al., 1995). By contrast, *Rgs2*, which was stalled but upregulated in G_0, showed a rapid decrease by 2 h of re-entry, and genes repressed in G_0 but not stalled (*Cdk1* and *Cdk6*) did not show rapid activation upon cell cycle re-entry (Fig. 3A; Fig. S5B,C). Furthermore, the rapid transcriptional surge during the G_0-G_1 transition was reflected in increased protein levels (for Ncl and Rps24; Fig. 3B; Fig. S5E) in both C2C12 myoblasts and primary MuSCs. These observations confirm that G_0-stalled repressed genes are functionally activated during the G_0-G_1 transition, and their common early reactivation is consistent with the hypothesis that reversal of stalling contributes to their coordinated restoration to transcriptional competence.

Transcriptional induction during the G_0-G_1 transition is associated with increased promoter clearance of RNAPII

We next investigated changes in promoter clearance of RNAPII from G_0 to early G_1 (from 30 min to 2 h of reactivation, the window of induced expression) by computing the SI for each candidate gene using targeted ChIP-qPCR. G_0-stalled repressed genes (*Ncl*, *Rps24*, *Ctdp1*, *Zc3h12A* and *Slbp*) exhibited highest SI in G_0, which decreased within 2 h of exit from quiescence, indicative of increased promoter clearance as the cells entered G_1 (Fig. 3C). By contrast, *Rgs2* (which showed stalled RNAPII but was transcriptionally active in G_0 cells) showed the opposite trend (i.e. increased SI in G_1), correlating with decreased expression. Thus, the change in SI between consecutive time points correlates inversely with change in expression and confirms that activation of G_0-stalled repressed genes is specifically accompanied by increased promoter clearance during the early G_1 transcriptional burst.

To assess whether global changes in RNAPII-dependent transcriptional activity occur during the exit from G_0, we quantified active phosphorylation marks on RNAPII (Fig. 3D,E). We observed a sharp increase in the proportion of Ser5-p- and Ser2-p-modified polymerase at the 30 min time point, indicating a rapid rise in transcriptional competence compared to G_0. These observations correlate well with the rapid rise of total RNA levels and active synthesis shown in Fig. 1B and C, which stabilize in 2 h. We conclude that G_0-stalled repressed genes undergo increased RNAPII promoter clearance upon exit from quiescence, which correlates with their rapid transcriptional induction during this transition.

Knockdown of G_0-specific targets of stalling is sufficient to induce features of quiescence in proliferating cells

Our observations thus far identified several G_0-specific repressed and stalled genes with the appropriate functions to participate in the biology of quiescence and activation. To investigate their potential role in establishment or maintenance of the quiescent state, we directly knocked down individual G_0-stalled genes (*Ctdp1*, *Ncl*, *Rps24*, *Slbp* and *Zc3h12A*) in MBs using siRNA (Fig. S6A,B) and evaluated effects on RNA synthesis, DNA synthesis and the cell cycle.

Total RNA content was significantly decreased in MBs treated with siRNA against *Ctdp1*, *Ncl*, *Rps24* and *Slbp* compared to levels in MBs treated with non-targeting siRNA control (Fig. 4A; Fig. S6C). Active RNA synthesis (as determined using EU incorporation assays) was also decreased upon knockdown of *Ctdp1*, *Ncl*, *Rps24* and *Zc3h12A* (Fig. 4A). Interestingly, nuclear area was also decreased in *Ctdp1*-, *Ncl*-, *Rps24*- and *Zc3h12A*-knockdown cells (Fig. 4A), which is consistent with the increased chromatin compaction seen in G_0 cells (Fig. S1A,C) (Everts et al., 2013). Notably, knockdown of three genes (*Ncl*, *Ctdp1* and *Rps24*) that are involved in RNA synthesis also led to reduced 5-ethynyl-2′-deoxyuridine (EdU) incorporation and G_1 arrest, whereas knockdown of two genes that affect posttranscriptional mechanisms of regulation (*Slbp* and *Zc3h12A*) did not result in significant changes in cell cycle profile (Fig. 4B; Fig. S6D). These genes regulate essential processes, and as expected, we observed ∼40% decrease in viability for *Rps24*-knockdown cells and ∼20% decrease in viability for *Ctdp1*- and *Ncl*-knockdown cells compared to ∼10% decrease in control siRNA-treated cells (Fig. S6E). Taken together, these observations demonstrate that in proliferating cells, repression of individual key genes that normally experience a G_0-specific repression and stalling is sufficient to trigger some quiescence-like features, as assessed by reduction in RNA content, active transcription and nuclear area.

To directly test the onset of quiescence in cells following knockdown of selected G_0-stalled repressed genes, we evaluated expression of quiescence-associated markers p27 (cyclin-dependent

Journal of Cell Science (2022) 135, jcs259789. doi:10.1242/jcs.259789

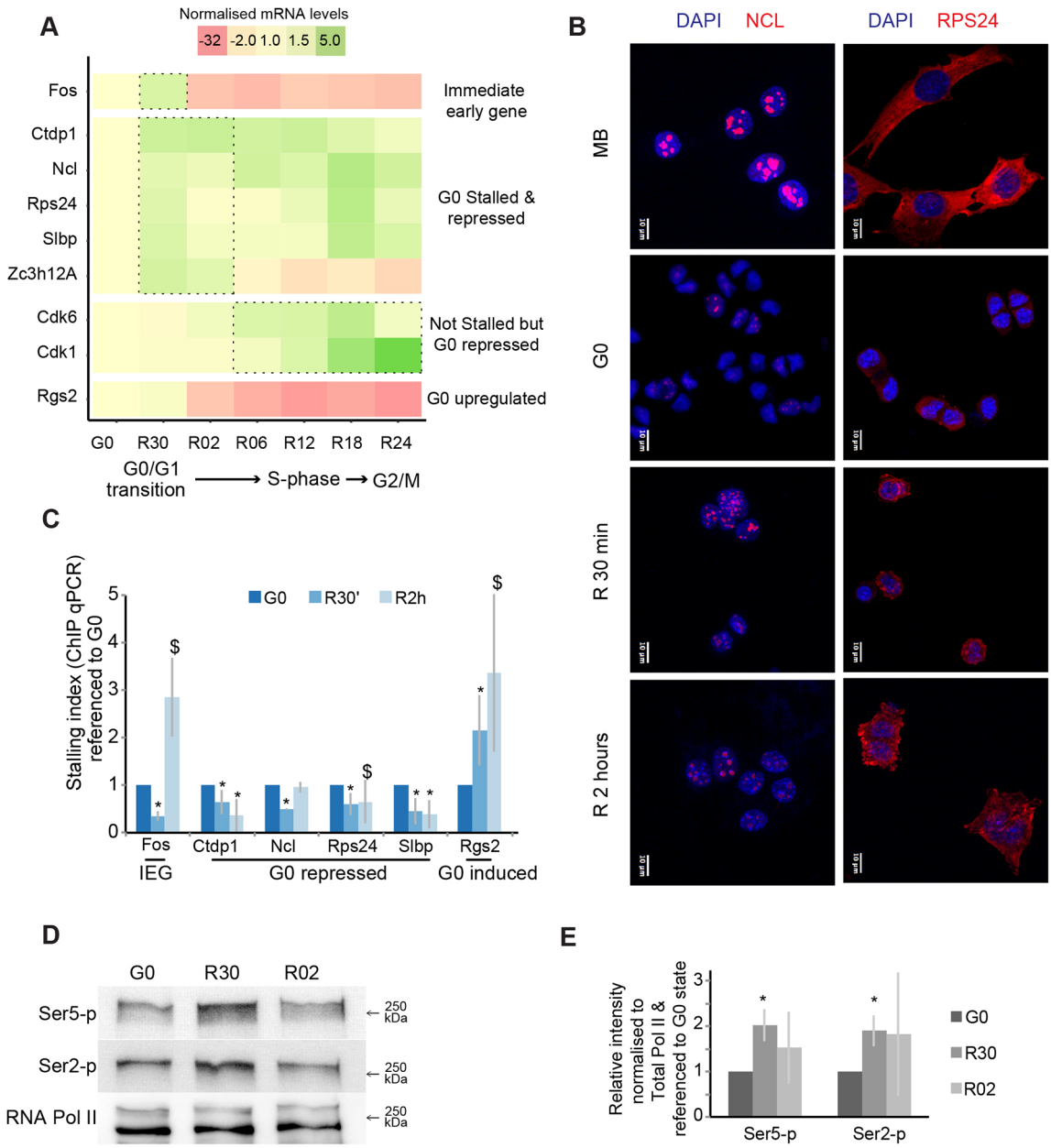

Fig. 3. G_0-specific stalled genes are repressed in quiescence and poised for activation. (A) RT-qPCR analysis of G_0-stalled genes (*Ctdp1*, *Ncl*, *Rps24*, *Slbp* and *Zc3h12A*) in quiescence and during cell cycle re-entry. Controls include *Fos* (an IEG), *Rgs2* (upregulated in G_0), *Cdk6* and *Cdk1* (both of which are repressed but not stalled in G_0 cells). Expression in all reactivation time points is normalized to expression in G_0, and the mean relative expression level is plotted versus time after exit from quiescence [30 min (R30′) to 24 h (R24)]. Cell cycle phases are indicated below the time points. Data are the mean of two experiments. (B) Proteins encoded by G_0-stalled genes are rapidly restored during cell cycle reactivation. Representative immunofluorescence images showing MBs, G_0 cells, and cells at 30 min (R30 min) and 2 h (R2 hours) after reactivation stained for proteins encoded by G_0-stalled genes (red) and DAPI (blue). Ncl protein (left) shows distinct nucleolar localization, whereas Rps24 (right) shows cytoplasmic localization. Expression is rapidly induced after reactivation. Images are representative of two experiments. (C) The SI of the indicated G_0-stalled genes decreases during cell cycle reactivation and is associated with expression dynamics. The SI was assayed using ChIP-qPCR and calculated as the ratio of ChIP enrichment for primers targeting the TSS versus the gene body (+500–1000 bp) at each time point: G_0, 30 min reactivation (R30′) and 2 h reactivation (R2h). Data are normalized to the SI in G_0 cells and are presented as the mean±s.d. of three experiments. *P<0.05; $ indicates 0.05<P<0.15 (two-tailed unpaired Student's *t*-test). (D,E) Activation of RNAPII during G_0-G_1 transition. (D) Western blots showing total RNAPII (RNA Pol II) and active phosphorylated forms in G_0 cells, and at 30 min (R30) and 2 h (R02) after reactivation. (E) Densitometric analysis of western blots as in D shows an increased proportion of Ser2-p and Ser5-p modifications by R30 compared to levels in G_0 cells, which is sustained at R02, correlating with cell cycle activation. Data are presented as the mean±s.d., n=3. *P<0.05 (two-tailed unpaired Student's *t*-test used).

kinase inhibitor 1B) (Oki et al., 2014) and p130 (retinoblastoma-family tumor suppressor, also known as RBL2) (Carnac et al., 2000; Litovchick et al., 2004) (Fig. S6F,G). Knockdown of *Ctdp1*, *Ncl* or *Rps24*, which resulted in reduced EdU incorporation, also resulted in a significant increase in the proportion of p27-positive cells that was comparable to the increase observed when proliferating cells were shifted to quiescence-inducing conditions (Fig. 4C). Similarly, p130 protein expression was induced when *Ctdp1*, *Ncl* or *Rps24* were knocked down in MBs (Fig. 4D). Since forced suppression of these RNA metabolism genes in proliferating cells

Journal of Cell Science (2022) 135, jcs259789. doi:10.1242/jcs.259789

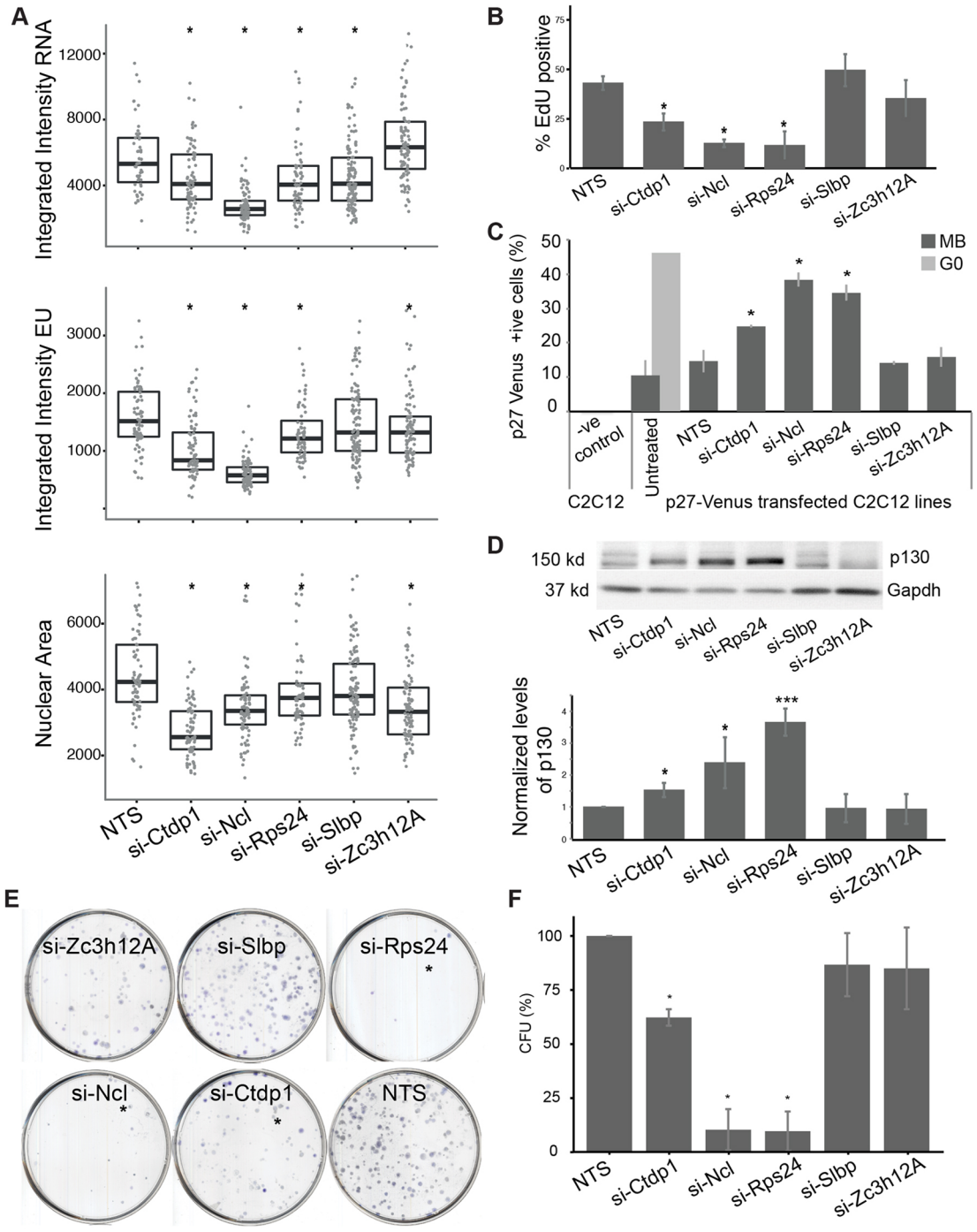

Fig. 4. Perturbation of G_0-stalled genes compromises the cell cycle and self-renewal. (A) Knockdown of G_0-stalled genes impacts RNA biogenesis. Total RNA levels (integrated intensity of SYTO Green, arbitrary units), EU incorporation (integrated intensity of EU, arbitrary units) and nuclear area (arbitrary units based on pixel counts) were quantified in MBs to estimate the effect of siRNA against the five selected genes (NTS, non-targeting control siRNA; representative images are shown in Fig. S6C). *n*>75 cells per condition pooled from three biological replicates. Boxplots show median values (horizontal bars) and the 25th to 75th percentile (boxes). **P*<0.05, *n*=3 (Mann–Whitney test). (B) Proliferation (S phase) of MBs was determined by measuring the percentage of cells that were EdU positive in an EdU incorporation assay. Proliferation is decreased after siRNA-mediated knockdown of *Ctdp1*, *Ncl* and *Rps24*. Data are presented as mean±s.d. of *n*=3. **P*<0.05 (two-tailed unpaired Student's *t*-test). (C) Induction of quiescence marker p27 in p27–mVenus MBs when expression of the indicated G_0-stalled genes was knocked down using siRNAs. Flow cytometry revealed an increase in the percentage of p27–mVenus-positive cells after knockdown of *Ctdp1*, *Ncl* and *Rps24* compared to the percentage in control cells (NTS, non-targeting siRNA). The negative (−ve) control sample represents untransfected C2C12 cells; the untreated samples show non-siRNA-treated p27–mVenus stable line during proliferation (MB) and quiescence (G_0) for comparison. Data are presented as the mean±s.d. of *n*=2. **P*<0.05 (compared to NTS; two-tailed unpaired Student's *t*-test used). (D) Induction of quiescence marker p130 protein levels (estimated using western blotting) in proliferating MBs when expression of the indicated G_0-stalled genes is knocked down using siRNAs. The knockdown of *Ctdp1*, *Ncl* and *Rps24* led to a significant increase in p130. Top: representative western blots. GAPDH is shown as a loading control. Bottom: normalized densitometry levels relative to the NTS control, presented as mean±s.e.m. of *n*=3. **P*<0.05; ****P*<0.001 (compared to NTS; two-tailed unpaired Student's *t*-test used). (E,F) siRNA-mediated knockdown of selected G_0-stalled genes affects self-renewal. (E) Representative images depicting reduced colony-forming ability of *Ncl*-, *Rps24*- and *Ctdp1*-knockdown MBs. Asterisks indicate significant change. (F) Quantification of clonogenicity [colony-forming units (CFU) expressed as a percentage of NTS control colonies]. Data are presented as mean±s.d. of *n*=3. **P*<0.05 (two-tailed unpaired Student's *t*-test used).

Journal of Cell Science

Journal of Cell Science (2022) 135, jcs259789. doi:10.1242/jcs.259789

was sufficient to induce markers typical of G_0, we suggest that their stalling-mediated repression contributes to the normal onset of quiescence.

G_0-stalled genes contribute to self-renewal

G_0 cells display enhancement of self-renewal compared to cycling cells, supporting the view that the quiescence program includes a self-renewal module (Collins et al., 2007; Subramaniam et al., 2013; Rumman et al., 2018). To investigate the role of G_0-stalled genes in self-renewal, we evaluated the effect of knockdown of such genes on clonogenic self-renewal. Knockdown of *Ctdp1*, *Ncl* or *Rps24*, which suppressed RNA synthesis and promoted G_1 blockade in proliferating cells, also resulted in a decrease in colony-forming ability compared with that of control cells (Fig. 4E,F). This finding further demonstrates the importance of timely reactivation of G_0-stalled genes during the G_0-G_1 transition, failure of which compromises self-renewal.

We conclude that repression of key cellular processes identified by analysis of G_0-specific RNAPII stalling is sufficient to cause cycling cells to acquire quiescence-like features. Consistent with the pre-existing transcriptional repression of G_0-stalled genes, further repression by siRNA knockdown does not appear to affect the quiescent state itself, but failure to de-repress expression upon quiescence exit (normally mediated by release of RNAPII stalling) results in attenuated cell cycle re-entry and diminished self-renewal.

Aff4, a component of the RNAPII SEC regulates G_0-stalled genes

Based on the findings described above, transcriptional output of G_0-stalled genes is repressed during quiescence and is rapidly upregulated during cell cycle re-entry. To gain insight into the mechanisms controlling expression of G_0-stalled genes, we screened known regulators of the transition from stalled to elongating RNAPII. Our targeted screen entailed knockdown of known regulators of RNAPII during quiescence and measuring expression of G_0-stalled genes, with de-repression as the discriminator. We selected the NELF complex, an inhibitor of elongation widely implicated in stalling (Gilchrist et al., 2008; Williams et al., 2015; Robinson et al., 2021), and three factors that

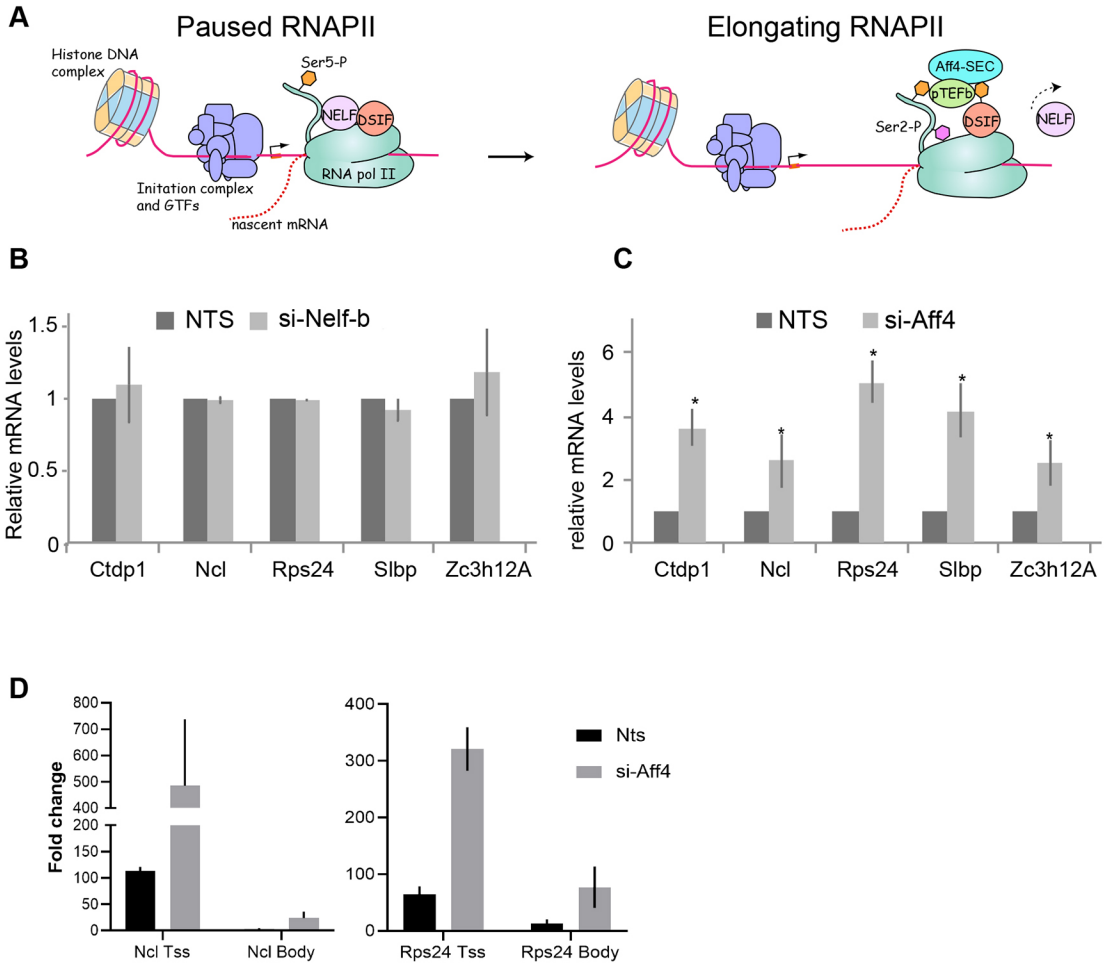

Fig. 5. Aff4, but not Nelf-b, regulates G_0-stalled genes. (A) Schematic representation depicting the composition expected in stalled versus elongating RNAPII (as reviewed by Kuehner et al., 2011; Margaritis and Holstege, 2008). GTFs, general transcription factors. (B,C) RT-qPCR analysis of expression of G_0-stalled genes in G_0 cells knocked down for (B) *Nelf-b* (si-Nelf-b) or (C) *Aff4* (si-Aff4), relative to expression in G_0 cells treated with non-targeting control siRNA (NTS). All five G_0-stalled repressed genes show significantly increased mRNA expression in *Aff4*-knockdown cells but not in *Nelf-b*-knockdown cells. Data are presented as mean±s.e.m. of n=3. *P<0.05 (two-tailed unpaired Student's t-test used). (D) ChIP-qPCR quantification of RNAPII occupancy on G_0-stalled genes (left, *Ncl*; right, *Rps24*) in G_0 cells treated with NTS or si-Aff4. RNAPII enrichment at the TSS and gene body of both G_0-stalled genes assayed is higher in si-Aff4-treated G_0 cells than in control NTS-treated G_0 cells, which is consistent with higher gene expression in *Aff4*-knockdown conditions. Data are presented as the mean±s.e.m. fold change (%) of input values relative to IgG control from $n\geq2$ experiments.

Journal of Cell Science (2022) 135, jcs259789. doi:10.1242/jcs.259789

regulate the availability and recruitment of P-TEFb – Hexim1, Brd4 and Aff4 (Fig. 5A,B; Fig. S7A) (Adelman and Lis, 2012; Jonkers and Lis, 2015). While Hexim1 regulates availability of P-TEFb, Brd4 and Aff4 help in its recruitment, and thereby assist in release of paused RNAPII. Based on the literature, we expected that knockdown of *Nelf-b* (which encodes a component of NELF complex; Narita et al., 2003) and *Hexim1* might lead to upregulation of G_0-stalled genes, whereas knockdown of *Brd4* and *Aff4* might lead to suppression of the selected G_0-stalled genes. However, knockdown of *Nelf-b* did not affect expression of G_0-stalled genes in the quiescent state (Fig. 5B). Knockdown of *Hexim1* led to downregulation of expression of four of the five genes tested (all except for *Ncl*) and Brd4 knockdown led to upregulation of *Ncl* and *Slbp* expression (Fig. S7B,C). Surprisingly, knockdown of *Aff4* led to significant upregulation of expression for all five selected G_0-stalled genes (Fig. 5C). Furthermore, RNAPII occupancy on both the TSS and gene body of G_0-stalled genes (*Rps24* and *Ncl*) was increased in the *Aff4* siRNA-treated G_0 cells, which is consistent with increased transcription from these loci (Fig. 5D). Although our targeted analysis does not indicate the extent of the role played by Aff4 in RNAPII stalling genome-wide, it does show gene-specific effects. Notably, we report an unexpected restraining role of Aff4 in G_0, distinct from other regulators of P-TEFb.

Since G_0-stalled genes are normally induced in G_1, we hypothesized that the upregulation of these genes in *Aff4*-knockdown cells might prime cells for accelerated cell cycle progression. Indeed, EdU incorporation during cell cycle re-entry (6 h and 12 h after G_0 exit) showed that Aff4 depletion uniquely led to accelerated S phase kinetics (~22% EdU-positive cells at 12 h compared to ~8% EdU-positive control cells). By contrast, the re-entry kinetics of cells treated with siRNA targeting *Nelf-b*, *Brd4* or *Hexim1* were unchanged (Fig. S7D). We validated the cell cycle kinetics of *Aff4*-knockdown cells using an extended time course of EdU incorporation, which confirmed an increased proportion of cells in S phase beginning at 12 h (Fig. 6A). Accelerated exit from G_0 for *Aff4*-knockdown cells was observed as early as 2 h after reactivation, as estimated using phosphorylation of RB1 at S795 (Rb p795), to assay the G_1-S transition (Fig. 6B). We further investigated the impact of knockdown of the different RNAPII modulators on self-renewal of G_0 cells. We observed that while *Nelf-b* knockdown did not affect colony formation, knockdown of other regulators (*Aff4*, *Brd4* and *Hexim1*) variably affected self-renewal (Fig. S7E,F).

To probe possible cell cycle stage-specific regulatory roles of Aff4 and Nelf-b, we knocked down these regulators in MBs and assayed for proliferation and differentiation (Fig. 6C,D). The results highlighted the opposing roles of Aff4 and Nelf-b: whereas knockdown of *Aff4* led to increased frequency of EdU incorporation (~15% higher proportion of EdU-positive cells compared to the proportion in the cells treated with non-targeting control siRNA) and no induction of myogenin (MyoG) expression, knockdown of *Nelf-b* did not alter EdU incorporation but led to an increased frequency of differentiation (20% MyoG-positive cells, compared to 1.7% in cells treated with non-targeting control siRNA). These observations lead us to conclude that in myoblasts (both proliferating and quiescent), Aff4 functions to restrain the cell cycle, as opposed to its established role as an inducer of proliferation in other tumorigenic cell lines (Deng et al., 2018). Interestingly, even though Aff4 protein levels were observed to be lower in G_0 cells than in MBs (Fig. S7G,H), Aff4 appeared to play similar roles in both states. We also conclude that Nelf-b exhibits a cell state-specific function in myoblasts, wherein it inhibits precocious differentiation in proliferating cells, but does not appear to affect the quiescent state.

In summary, our results demonstrate cell cycle stage-specific changes in transcriptional activity at the level of global RNA synthesis and RNAPII modifications associated with active transcription. Although quiescent cells exhibit global transcriptional repression, only genes involved in RNA metabolism (but not cell cycle or myogenic differentiation) are maintained in a transcriptionally poised state during quiescence. This poising mechanism maintains quiescence-specific repression of a network of target genes and enables rapid transcriptional activation essential for timing and efficiency of cell cycle re-entry. Promoter-proximal RNAPII stalling contributes to this transcription-poising mechanism, and we uncover an unexpected role of the SEC component Aff4 in restraining gene expression and the G_0-G_1 transition (Fig. 7).

DISCUSSION

In this study, we investigated the mechanisms involved in quiescence-associated global transcriptional repression. While mitotic inactivity is known to be associated with reduced transcription, mechanisms focused on RNAPII have been less well explored. We now report that RNAPII localization and expression levels, as well as the extent of repression of global RNA content and synthesis, differ quantitatively between reversibly and irreversibly arrested states. The availability of RNAPII is tightly regulated in G_0, and regulators of RNA biogenesis are among the most strongly repressed genes in reversibly arrested cells. Strikingly, promoter-proximal RNAPII pausing is enhanced on state-specific sets of genes. Loci encoding regulators of RNA biogenesis experience prominent RNAPII pausing in G_0, and release of pausing on these genes is critical for the G_0-G_1 transition. Unexpectedly, we uncovered a role for the SEC component Aff4 as a regulator of RNAPII pausing in quiescence. We conclude that RNAPII activity and stalling contribute to transcriptional repression that controls quiescence, and that transcriptional induction of G_0-stalled genes is required for competence for proliferation and self-renewal.

Revisiting the transcriptome of quiescent cells using RNA-seq reveals major differences in RNA biogenesis compared to that in permanently arrested cells

Using genome-wide comparative analysis that assumes equivalent RNA content across samples, studies of cultured and primary cells have identified a quiescence signature (Coller et al., 2006; Fukada et al., 2007; Liu et al., 2013; Hausburg et al., 2015). However, our study clearly shows that altered RNA metabolism in G_0 myoblasts leads not only to lower RNA synthesis but also to strongly reduced total RNA content per cell. This led us to re-evaluate the transcriptome of quiescent cells using RNA-seq, followed by normalization of transcript levels to equal cell number rather than equal RNA. A major insight from this analysis is that a much larger number of genes are strongly repressed than was previously appreciated, bringing the repression of regulators of RNA biogenesis into sharp focus. Interestingly, these pathways are not repressed in differentiated cells, which is consistent with the observations that RNAPII regulation distinguishes two mitotically inactive states, suggesting distinct global control mechanisms in the two modes of cell cycle exit. A striking finding of this analysis comparing the new C2C12 datasets with RNA-seq data from *in vivo* fixed MuSCs (Yue et al., 2020) is that induced quiescence in cultured

Journal of Cell Science (2022) 135, jcs259789. doi:10.1242/jcs.259789

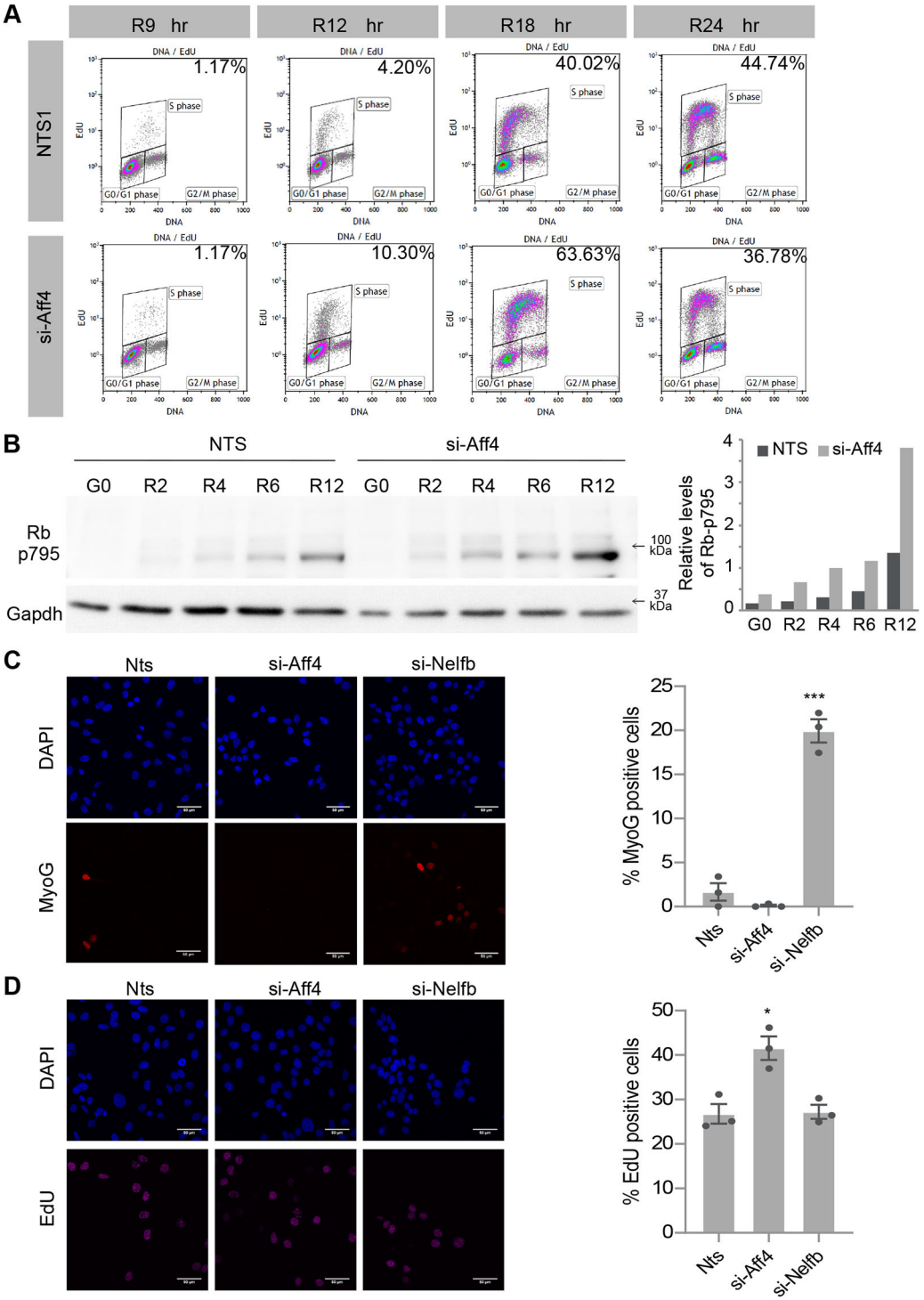

Fig. 6. Cell cycle stage-specific roles of Aff4 in regulating G_0-G_1 transition and proliferation. (A) *Aff4* knockdown hastens S phase. Flow cytometry horseshoe plots of EdU-pulsed cells during a cell cycle re-entry time course (9–24 h of re-entry from G_0, R9–R24), showing the percentage of S-phase cells in *Aff4*-knockdown (si-Aff4) and control cells (treated with non-targeting siRNA, NTS1) at each time point. Cells were co-stained for DNA (*x* axis) and EdU (*y* axis). The percentage of S-phase cells (inset) is substantially higher at 12–18 h in the *Aff4*-knockdown population. Data shown are representative of one experiment. (B) Cell cycle re-entry is accelerated in *Aff4*-knockdown cells compared to cells treated with non-targeting control siRNA (NTS). Western blot (left) shows that an early marker for G_1-S transition – phosphorylation of RB1 at S795 (Rb p795) – is activated earlier and to higher levels in *Aff4*-knockdown cells than in control cells, indicating that *Aff4* knockdown speeds up reactivation. Rb p795 levels in G_0 and during a time course of re-entry (2–12 h, R2–R12) are shown, with GAPDH used as a loading control. Densitometric quantification of relative Rb p795 levels is shown on the right. Data are representative of one experiment. (C) Differentiation is induced in MBs 48 h after knockdown of *Nelf-b* (si-Nelfb), but not after knockdown of *Aff4*, as assayed by myogenin staining (red). DNA was stained using DAPI (blue). Representative immunofluorescence images (left) and quantification (right) are shown. (D) EdU incorporation was enhanced in MBs 48 h after knockdown of *Aff4*, but not after knockdown of *Nelf-b*. Representative immunofluorescence images (left) and quantification (right) are shown. In C and D, non-targeting control siRNA (Nts) was used as a control, and more than 300 cells were counted per sample across n=3 experiments. Data are presented as mean±s.e.m. *$P \leq 0.05$; ***$P \leq 0.001$ (two-tailed unpaired Student's *t*-test). Scale bars: 50 µm.

Journal of Cell Science (2022) 135, jcs259789. doi:10.1242/jcs.259789

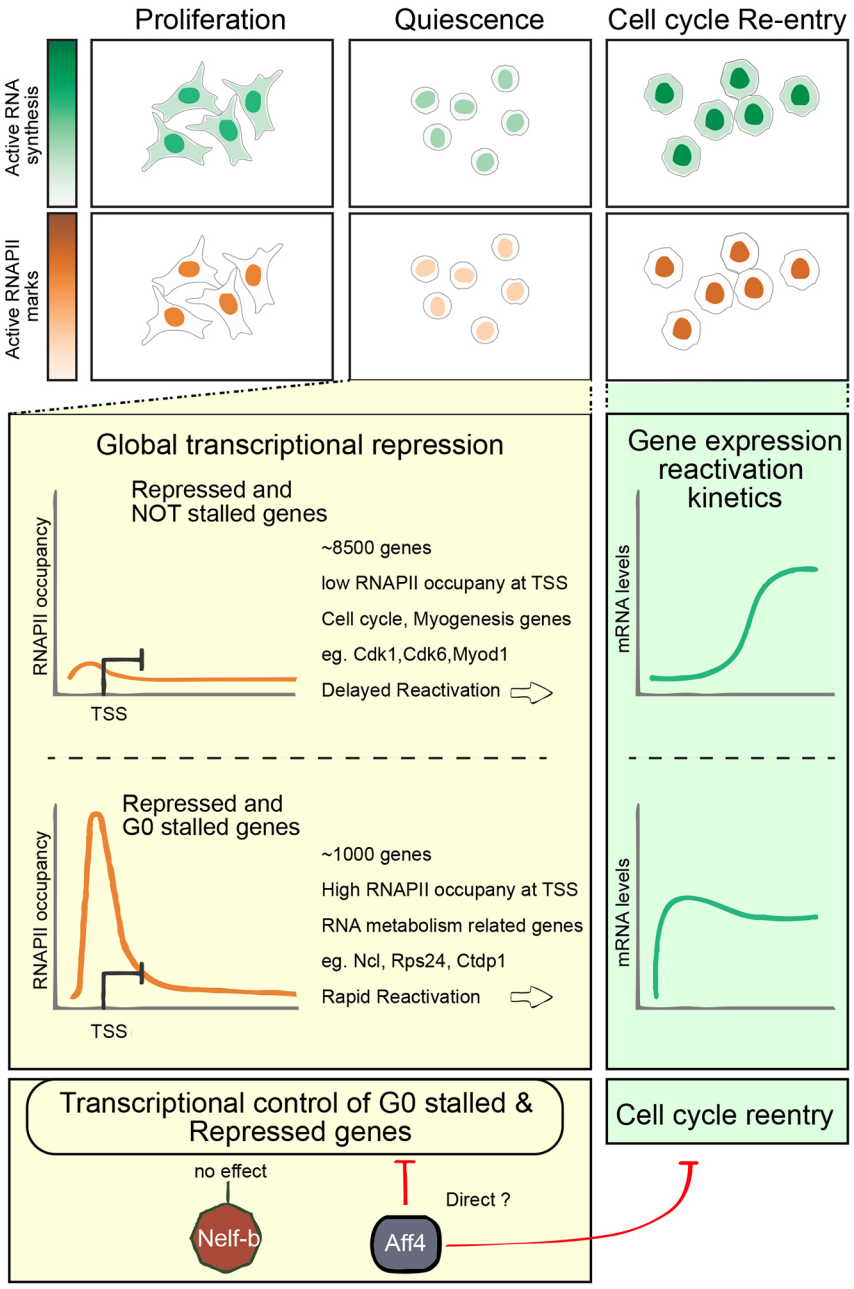

Fig. 7. RNAPII pausing in regulation of quiescence – a new role for Aff4 in restraining the G_0-G_1 transition. Global transcriptional repression in quiescence is associated with reduced levels of both total and active RNAPII. However, a subset of repressed genes, mostly associated with RNA metabolism, exhibit prominent RNAPII occupancy at their promoters. Release of this promoter-proximal pausing allows these genes to activate early as compared to other repressed genes, and thereby sets the timing for coordinated cellular activation and entry into the cell cycle. Interestingly, regulators of RNAPII pause-release exhibit cell state-specific functions: Nelf-b does not appear to affect quiescence maintenance and activation, whereas Aff4 plays a significant role in restraining expression of G_0-stalled genes and premature cell cycle entry.

myoblasts captures the quiescence signature of unperturbed MuSCs *in vivo*.

RNAPII transcriptional machinery distinguishes reversible and irreversible arrest

Reduced transcriptional output is typical of cells whose proliferative activity has slowed, as has been shown in many systems (Bertoli et al., 2013) including quiescent adult stem cells (Freter et al., 2010). Here, we observed several notable differences in RNAPII activity as MBs withdrew into alternate arrested states to become either G_0 cells or MTs. We found that reversibly arrested G_0 cells exhibit reduced nuclear and active RNAPII levels compared to those in terminally arrested MTs. Despite lower total levels of RNAPII protein, and increased exclusion from the nucleus, the extent of RNAPII stalling was higher in quiescence. Moreover, it is the G_0-specific repressed genes that show promoter proximal RNAPII pausing and regulation by a mechanism that is apparently NELF-independent (at least for three selected genes – *Ctdp1*, *Ncl* and *Rps24*).

Quiescence-repressed genes are poised for activation in G_1

An important hallmark of quiescent cells concerns their extended kinetics of S-phase re-entry compared to that of a continually cycling population. This additional phase – the G_0-G_1 transition – has long been appreciated to integrate extracellular signaling (Pledger et al., 1978), but the regulation of its duration is still incompletely understood (Coller, 2007). Recent studies in MuSCs have captured this transient phase, or ‘G-alert’, by compromising mTORC1 activity (Rodgers et al., 2014), suggesting key inputs by signaling that activates global translation. Our study suggests that transcriptional control by RNAPII pausing and its reversal may also play a role in determining kinetics of the G_0-G_1 transition. The rapid

Journal of Cell Science (2022) 135, jcs259789. doi:10.1242/jcs.259789

activation of G_0-stalled repressed genes (particularly regulators of RNA biogenesis) preconfigures changes in cellular processes that are essential for cell cycle re-entry. Transcriptional activation associated with cell cycle re-entry is accompanied by loss of RNAPII stalling, increased active RNAPII phosphorylation marks (Ser2-p and Ser5-p) and a rapid burst in active RNA synthesis very early in G_1. The timing of these events suggests that the increase in active RNAPII marks is linked to the exit from quiescence. We suggest that release of polymerase stalling and the burst of active transcriptional output during reversal of quiescence promotes cell cycle entry and fine-tunes the transcriptional cascade required for de-repressing a variety of cellular processes essential for progression from G_0 to G_1 to S phase.

Repression of G_0-stalled genes contributes to blocked proliferation and sustained self-renewal

G_0-stalled genes identified in this study (*Ctdp1*, *Ncl*, *Rps24*) have been suggested to possess tumor suppressive properties in other systems (Badhai et al., 2009; Ugrinova et al., 2007; Zhong et al., 2016). Interestingly, the yeast ortholog of *Ctdp1*, *FCP1*, which controls the restoration of active RNAPII during the transcription cycle, was previously identified in a genetic screen for quiescence-regulatory genes (Sajiki et al., 2009). Furthermore, in mammalian cells, Ctdp1 has been implicated in controlling global levels of polyA transcripts as well as in rapid induction of heat shock genes (Fuda et al., 2012; Cho et al., 2001; Kobor et al., 1999; Mandal et al., 2002), both of which are functions ascribed to RNAPII-mediated transcriptional regulation. Thus, stalling-mediated control of the *Ctdp1* gene itself and its reduced expression in G_0 may suggest a feed-forward mechanism by which RNAPII activity is further depressed in G_0. The products of the ribosomal machinery genes *Ncl* and *Rps24* are involved in the very first processing step that generates pre-rRNA (Choesmel et al., 2008; Ginisty et al., 1998). *Rps24* mutations result in Diamond–Blackfan Anemia, which is characterized by ribosome biogenesis defects in hematopoietic stem cells and erythroid progenitors (Choesmel et al., 2008; Song et al., 2014), thereby suggesting an important role for ribosomal proteins in maintenance of progenitor functions. RNAPII stalling-mediated regulation in G_0 (as identified in this study) is thus indicative of regulatory programs that keep the major biosynthetic pathways in check to maintain the quiescent, stem-like state.

Expression of G_0-stalled genes is not contingent on NELF

Promoter-proximal RNAPII stalling has been shown to involve the NELF complex, which associates with the DSIF complex to inhibit progression of the transcription initiation complex to productive elongation (Yamaguchi et al., 1999). However, in our study, knockdown of *Nelf-b* during quiescence did not alter expression of stalled genes, suggesting that promoter-proximal stalling in G_0 is independent of Nelf-b. It is plausible that quiescence-specific regulation of G_0-stalled genes is similar to RNAPII 'docking' mechanisms observed in the diapause arrested state in *Caenorhabditis elegans*, which lacks the NELF complex (Maxwell et al., 2014). Moreover, our finding aligns closely with a recent report that implicates Nelf-b specifically in muscle progenitor expansion *in vivo* via modulation of pigment epithelium-derived factor (PEDF) and p53 pathways, but not in quiescent or differentiating cells (Robinson et al., 2021). In that study, MuSC-specific knockout of *Nelf-b* did not affect maintenance of quiescence and activation, or muscle homeostasis, but did compromise muscle regeneration overall, suggesting a cell state-specific role. Furthermore, depletion of Nelf-b in proliferating MuSCs resulted in disregulation of a limited number of genes. Notably, the study in MuSCs implicated stalling by the evaluation of nascent genome-wide transcription, and suggests a more restricted role of this transcription factor than previously believed. Our results in cultured myoblasts are consistent with the findings of Robinson et al. (2021) *in vivo*, in that knockdown of *Nelf-b* in cycling myoblasts reduced proliferation and increased differentiation markers, whereas knockdown during quiescence had no effect on transcription of G_0-stalled genes and self-renewal. Taken together, our results support the view that quiescence-specific, NELF-independent mechanisms control transcription of G_0-stalled genes.

The SEC component Aff4 emerges as a regulator of G_0-stalled genes, controlling the timing of S-phase entry

While quiescence is known to involve repressed transcription, G_0-specific regulation of RNAPII has not been previously reported. The notion that regulators of stalling, such as the DSIF and NELF complexes, participate in all cellular states has been challenged by a recent report studying MuSCs *in vivo* (Robinson et al., 2021) and by our own analysis (see above). We investigated specific components of the P-TEFb regulatory system complex as good candidates for the release of stalling of specific target genes during G_1 (Lu et al., 2016). Release of stalled RNAPII is brought about by coordinated regulation of P-TEFb mediated by the SEC, Brd4 and Hexim1 (Lu et al., 2016; Puri et al., 2015). Hexim1 haplodeficiency in mice increases MuSC activity and muscle regeneration, highlighting a role in self-renewal (Galatioto et al., 2010). In our culture model, *Hexim1* knockdown did not affect the timing of cell cycle re-entry, but an effect in G_0 cannot be ruled out, and the observed repression of some G_0-stalled genes warrants further investigation.

The pause-release regulator that had the most interesting phenotype in our study was Aff4, considering that it is generally thought to promote cell proliferation (Deng et al., 2018). As a component of the SEC, Aff4 is known to display target gene specificity (Luo et al., 2012), promoting release of paused RNAPII on heat shock genes and *MYC* (Kühl and Rensing, 2000; Luo et al., 2012; Schnerch et al., 2012). Indeed, preventing induction of oncogene transcription by Aff4 is a therapeutic avenue in cancer (Hu et al., 2021; Katagi et al., 2021; Wu et al., 2021), and inactivation of Aff4 in mesenchymal stem cells has pro-proliferative and anti-differentiation effects (Zhou et al., 2017). In our study of myoblasts, *Aff4* knockdown led to more rapid transition from G_0 to G_1, along with higher proliferation and reduced differentiation, supported at a molecular level by enhanced expression of G_0-stalled genes. Interestingly, although Aff4 has been considered a positive regulator of RNAPII, knockdown studies in HEK cells have shown upregulation of a small number of genes (Luo et al., 2012), indicating that Aff4 might normally restrain some target genes in other cell types as well. Comparison of the GO terms assigned to these upregulated genes with those assigned to the G_0-stalled genes identified in our study shows similarities in several classes, including RNA metabolism and mRNA processing [Luo et al. (2012) versus this study, data not shown]. While the mechanism of repression (direct or indirect) remains unknown at present, we infer that Aff4 mediates differential regulation (activation or repression) of its target genes. In our study, *Aff4*-knockdown cells show accelerated entry from G_0 to S phase, indicating that Aff4 action on a subset of target genes guards against premature activation of quiescent cells, regulating the timing of cell state transitions.

In conclusion, this study identifies control mechanisms that allow establishment, maintenance and timely release of a transcriptionally repressed quiescence program. During quiescence, although the

Journal of Cell Science (2022) 135, jcs259789. doi:10.1242/jcs.259789

nuclear RNAPII pool is reduced compared to that in proliferating cells, many promoters of genes controlling RNA metabolism are occupied but not active. We uncover a repressive role for RNAPII pausing in the control of RNA metabolic genes that contributes to entry into quiescence, and we highlight a role for the SEC regulator Aff4 in establishment and/or maintenance of the quiescent state. Overall, this study extends the role of RNAPII pausing in regulating not only developmental lineage transitions (Scheidegger and Nechaev, 2016) but also cell cycle transitions, and in particular, sheds light on the reversible arrest typical of adult stem cells.

MATERIALS AND METHODS

Cell culture

C2C12 myoblasts were obtained from Helen Blau (Stanford University, CA, USA), and a sub-clone A2 (Sachidanandan et al., 2002) was used in all experiments. Proliferating C2C12 myoblasts (MBs) were maintained in growth medium [GM; DMEM (Gibco) with 20% fetal bovine serum (FBS; Gibco) and 1% penicillin-streptomycin (Gibco)] and were passaged at 70–80% confluency.

Differentiation into myotubes (MTs) was induced when MBs reached 80% confluence after washing with phosphate-buffered saline (PBS) and addition of differentiation medium [DM; DMEM with 2% horse serum (HS; Gibco)], which was replaced daily for 5 d. Multi-nucleated MTs began to appear after 24 h in DM. Quiescence induction by suspension culture of MBs was as described previously (Sachidanandan et al., 2002), where sub-confluent cultures were trypsinized and cultured as a single-cell suspension at a density of 10^5 cells/ml in semi-solid medium [DMEM containing 1.3% methyl cellulose (Sigma), 20% FBS, 10 mM HEPES and 1% penicillin-streptomycin (Gibco)]. After 48 h, when ∼98% of cells had synchronized in G_0, arrested cells were harvested by centrifugation (following dilution of the methyl cellulose-containing medium with PBS) and, where indicated, were reactivated by plating at a sub-confluent density in GM before being collected at defined times (30 min to 24 h).

Colony formation assay

Cells were counted three times (at two or more dilutions) using Trypan Blue (Thermo Fisher Scientific) exclusion to generate an accurate live-cell count using a Countess Automated Cell Counter (Invitrogen). Next, 500 live cells were replated in GM on 150 mm dishes in triplicate. After 7 d of culture, colonies were fixed with 70% ethanol, stained with 1% Methylene Blue (Sigma) and counted.

Muscle fiber isolation and culture

Animal work was conducted at NCBS/inStem Animal Care and Resource Center and the CCMB Animal Facility. All procedures were approved by inStem and CCMB Institutional Animal Ethics Committees following norms specified by the Committee for the Purpose of Control and Supervision of Experiments on Animals, Government of India.

Single muscle fibers were isolated and cultured using the Anderson lab method (Leiter and Anderson, 2010; Anderson et al., 2012) with some modifications (Shefer and Yablonka-Reuveni, 2005; Siegel et al., 2009). Briefly, extensor digitorum longus (EDL) muscle was dissected from 8–12-week-old Tg:Pax7–nGFP mice (a kind gift from Shahragim Tajbakhsh, Institut Pasteur, Paris, France; Sambasivan et al., 2009). Isolated muscles were digested with type I collagenase (Worthington) in DMEM at 37°C for ∼45 min. Dissociated fibers were transferred into fresh DMEM medium and triturated to release individual fibers using fire-polished Pasteur pipettes. Fibers were cleaned by multiple media washes and transferred to fiber culture medium [DMEM (Gibco), 20% FBS (Gibco), 10% HS (Gibco), 2% chick embryo extract (GENTAUR), 1% penicillin-streptomycin (Gibco) and 5 ng/ml bFGF (Sigma)].

For quantification of active RNA synthesis, 5 mM EU (Thermo Fisher Scientific) was added to the medium followed by detection as described below. For immunostaining, freshly isolated or cultured single fibers were fixed in 4% PFA for 5 min, washed three times with PBS, and picked and placed on charged slides (Thermo Fisher Scientific) for antibody detection.

Knockdown of target genes using RNAi

C2C12 cells were cultured in GM until 80% confluent before being trypsinized. Then, ∼0.3×10^6 cells were plated on 100 mm dishes for 12–14 h before being transfected with siRNA [145 pM of siRNA SMARTpool (Dharmacon) mixed with 43 µl Lipofectamine RNAiMAX (Invitrogen)] and incubated with siRNA–lipid complex for 24–48 h. The extent of knockdown was evaluated using RT-qPCR and western blotting before further experimental analysis. Transfection reactions were scaled up or scaled down according to the manufacturer's protocol. Typically, siRNA-mediated knockdown of 50–90% reduction at RNA level was obtained. siRNAs used in this study are detailed in Table S1.

Immunofluorescence and microscopy

Cells plated on coverslips or harvested from suspension cultures were washed with PBS, fixed in 2% PFA at room temperature (RT) for 20 min, permeabilized and blocked in PBS containing 10% HS and 0.5% Triton X-100 (blocking buffer). Primary antibodies (Table S2) were diluted in blocking buffer. Secondary antibody controls were negative – no cross reactivity of secondary reagents was detected. For total RNA quantification, fixed cells were incubated with 10 µM SYTO RNASelect (Invitrogen) for 30 min. For detection of DNA and RNA synthesis, cells were pulsed for 30 min with EdU (10 µM concentration; Invitrogen) or EU (5 mM concentration), respectively, and fixed with 2% PFA for 20 min at RT. Labeling was detected using a Click-iT imaging kit (Invitrogen), as per the manufacturer's instructions. Samples were mounted in aqueous mounting agent with DAPI (Vector Laboratories) and imaged on a Leica TCS SP8 confocal microscope (63× objective, 1.4 NA). Minimum global changes in brightness or contrast were made, and composites were assembled using Image J (NIH, Bethesda, MD). The automation of intensity calculation and counts was carried out using a custom pipeline created on the CellProfiler platform (Carpenter et al., 2006; Kamentsky et al., 2011).

Cell cycle analysis using flow cytometry

RNA and DNA content

Adherent cells were trypsinized, washed in PBS and pelleted by centrifugation. Suspension-arrested cells were recovered from methyl cellulose treatment as described above. Cell pellets were dispersed to single cells by trituration in 0.75 ml of PBS, and the cells were then fixed by dropwise addition into 80% ice-cold ethanol with gentle stirring. Following fixation (cells could be stored up to 7 d at −20°C), cells were briefly washed with PBS and resuspended in PBS at 1 million cells per 500 µl PBS containing 40 µM DRAQ5™ (DR50050, Biostatus) and 10 µM SYTO RNASelect (S-32703, Invitrogen). Cell cycle analysis was performed on a FACS Caliber cytometer (Becton Dickinson) to assay DRAQ5™ (wide range of absorption, emission maximum at 697 nm) and SYTOX Green (absorption/emission maxima of ∼490/530 nm). In total, 10,000 cells were analyzed per sample. CellQuest software (Becton Dickinson) was used for acquisition and FlowJo (Becton Dickinson) was used for analysis.

EdU and propidium iodide analysis

Cells were pulsed with EdU and fixed as described above, washed twice in PBS and resuspended in propidium iodide (PI) staining solution (50 µg/ml PI and 250 µg/ml RNaseA) for 30 min in the dark. For analysis of S-phase cells during cell cycle re-entry, EdU-pulsed cells were fixed in 4% PFA for 10 min, then washed and stored in PBS at 4°C. For staining, cells were permeabilized and blocked in PBS containing 10% FBS and 0.5% Triton X-100, and labeling was detected using a Click-iT imaging kit (Invitrogen) as per the manufacturer's instructions. Cells were co-stained with PI (50 µg/ml, with 250 µg/ml RNaseA) and analyzed on Gallios cytometer (Beckman Coulter). Kaluza software (Beckman Coulter) was used to acquire and analyze the data.

Quiescence estimation by p27–mVenus reporter assay

A C2C12 reporter line stably expressing p27–mVenus [a G_0 marker created by fusing a defective mutant of the p27 CDK inhibitor, p27K(−), with mVenus; Oki et al., 2014] was generated by transfection and antibiotic

selection. Adherent MBs expressing p27–mVenus with or without knockdown of various G_0-stalled genes were trypsinized and fixed in 4% PFA for 10 min at RT. G_0 cells were recovered from suspension as described above and fixed as for MBs. Fixed cells were analyzed for mVenus expression (excitation, 515 nm; emission, 528 nm) using a Gallios flow cytometer (Beckman Coulter). Kaluza or FlowJo software was used to acquire and analyze the data.

Western blot analysis

Lysates were obtained from adherent or suspension cultures (2×10^6 cells). PBS-washed cells were harvested by centrifugation and resuspended in 500 µl of lysis buffer (2× SDS lysis buffer, pH 6.8). Protein amount in lysates was estimated using Amido Black (Sigma) staining and quantification of absorbance at 630 nm. Proteins were resolved on 8% acrylamide gels and transferred to PVDF membrane (Bio-Rad), incubated with primary antibody overnight at 4°C, washed in Tris-buffered saline (TBS) containing 0.1% Tween 20 (TBS-T) for 10 min, followed by incubation with secondary antibody conjugated to horseradish peroxidase (HRP) for 1 h. After a 10 min wash with TBS-T, HRP activity was developed using ECL reagent (Bio-Rad) and chemiluminescent detection (Vilber Lourmat). Details of antibodies and dilutions used are given in Table S2.

Isolation of RNA from cultured cells and RNA sequencing library preparation

For accurate determination of cell number in different states, attached cultures or suspension cells were counted three times (at two or more dilutions) using Trypan Blue exclusion to generate a live-cell count using a Countess Automated Cell Counter (Invitrogen). Accurate counts were not possible for MT samples because the multi-nucleate nature of the cells meant that cells with varying number of nuclei were present; therefore, nuclei were isolated and counted to represent cell counts for these samples.

Cells were washed twice with cold PBS, then lysed using 1 ml RLT Plus buffer containing β-mercaptoethanol (RNeasy Plus Mini Kit, Qiagen). The resulting lysate was vortexed vigorously to shear genomic DNA then stored at −70°C until RNA was isolated using an RNeasy Plus Mini Kit (catalog no 74134, Qiagen), as per the manufacturer's protocol, using an RNeasy MinElute spin column. RNA was eluted from the column twice, with each elution using 30 µl of water, then quantified using a NanoDrop ND-1000UV-Vis spectrophotometer (NanoDrop Technologies, Wilmington, DE), and checked by gel electrophoresis and q-RT PCR for marker transcripts. For RNA-seq, RNA quantification and quality check was done using an Agilent RNA 6000 Pico Kit on Agilent 2100 Bioanalyzer system.

RNA sequencing libraries were prepared from duplicate MB, G_0 and MT samples. By quantifying an exogenously added 'spike-in' RNA mix, each of the six libraries were referenced to RNA content per million cells, correcting for sampling biases generated during sequencing. To achieve this, 3 µl per million cells of ERCC spike-in RNA mix (1:10 dilution; Thermo Fisher Scientific, 4456740; https://assets.thermofisher.com/TFS-Assets/LSG/manuals/cms_095046.txt) was added to each sample. Since the RNA-seq experiment was carried out in duplicate, ERCC mixes were added to distinguish each replicate set (MB, MT, G_0): mix 1 was added for MB_1, MT_1 and G_0_1 replicates; and mix 2 was added for MB_2, MT_2 and G_0_2 replicates. The spiked total cellular RNA was DNase treated to remove traces of DNA (DNA-free kit; Ambion, AM1906), and 4 µg of DNase-treated spiked RNA was processed to remove ribosomal RNA (RiboMinus Eukaryotic kit V2; Ambion, A15020). Quality of Ribominus-treated RNA was checked on a BioAnalyzer. Finally, the purified mRNA was used for cDNA synthesis and library preparation using an NEBNext Ultra Directional RNA Library Prep Kit for Illumina (New England Biolabs, E7420). The library thus prepared was quality checked on a BioAnalyzer and verified by qPCR for marker transcripts prior to carrying out paired-end sequencing on an Illumina HiSeq1000.

ChIP and ChIP-seq library preparation

Cell harvesting and sonication

Wild-type C2C12 cells (8×10^6) were harvested in cell dissociation buffer (Sigma), collected in 15 ml tubes and washed with PBS. Cell pellets were resuspended in GM containing a final concentration of 1% HCHO (Sigma). Cells were incubated for 10 min at 37°C followed by two washes with cold PBS and finally were lysed in 1.6 ml of SDS lysis buffer (1% SDS, 10 mM EDTA and 50 mM Tris-HCl, pH 8.1). Lysates were incubated on ice for 20 min and spun at 13,500 ***g*** for 10 min at 4°C. Then, 200 µl samples of the supernatant were subjected to sonication for 60 s on/off for 16 cycles for G_0 and MB samples, and 18 cycles for MT samples (Bioruptor sonicator). Aliquots of chromatin samples were stored at −80°C. Two replicate samples of G_0 cells, MBs and MTs were prepared for ChIP and subsequent sequencing.

Immunoprecipitation

A ChIP Assay Kit (Millipore, 17-295) was used to carry out immunoprecipitation as per the manufacturer's protocol. Briefly, 200 µl samples of sonicated lysates were diluted to a 2 ml total volume by adding ChIP dilution buffer and then pre-cleared with Dynabeads™ Protein A beads (Thermo Fisher Scientific; agarose beads from the ChIP Assay Kit were not used). Cleared supernatants were recovered and incubated with 7.5 µg antibody (anti-Rbp1 to detect total RNAPII; N20 clone, rabbit IgG) for 16 h at 4°C on a rotary shaker. Dynabeads Protein A/Protein G (Thermo Fisher Scientific) were added to collect immune complexes. Washes (1 ml) in a series of buffers were performed as follows: low salt immune complex wash buffer, high salt immune complex wash buffer, LiCl wash buffer, and two washes in TE (10 mM Tris-HCl and 1 mM EDTA). All washes were done at 4°C on a rotary shaker for 5 min each and collected by magnetic separation. Finally, the beads were resuspended in 250 µl freshly prepared elution buffer (1% SDS, 0.1 M $NaHCO_3$) and incubated at RT for 15 min. The elution process was repeated twice, and 20 µl of 5 M NaCl was added to 500 µl of combined eluate for reverse crosslinking at 65°C for 16 h. Reverse-crosslinked eluates were digested with 2 µl of 10 mg/ml proteinase K (Thermo Fisher Scientific) at 45°C for 1 h. Qiagen nucleotide removal kit was used to purify DNA. Purified DNA was subjected to real-time PCR with primers as shown in Table S3. Each DNA sample was analyzed in triplicate, in at least three independent experiments.

ChIP-seq library preparation

For sequencing library preparation, 20 ng samples of ChIP pulldown DNA and input DNA were used with an NEBNext DNA Library Prep kit for Illumina (New England Biolabs, E6000) along with NEBNext Multiplex oligos for Illumina (index primers set 1; New England Biolabs, E7335), as per the manufacturer's protocol. The library thus prepared was quality checked on a BioAnalyzer and by qPCR prior to carrying out paired-end sequencing on an Illumina HiSeq1000.

Sequencing data analysis

Sequenced RNA-seq libraries were aligned to the *Mus musculus* reference genome (mm9 build with 92 spike-in mRNA sequences added as pseudo-chromosomes) using TopHat (version 2.0.10). Reference annotation version M1 (gtf file from July 2011 freeze; NCBIM37 Ensembl release 65 from the GENCODE consortium) along with ERCC transcripts was used. For equal RNA normalization, Cufflinks (2.1.1 version) was used for transcript abundance and differential expression analysis (Cuffdiff; Trapnell et al., 2012). CummeRbund (2.6.1 version; http://compbio.mit.edu/cummeRbund/) was used for sub-selection of differentially expressed gene list (Tables S4–S6). For equal cell number normalization, the HTseq-count package (0.54 version; Anders et al., 2015) was used to quantify reads per gene for each of the samples using the reference annotation file. This was further normalized using the DEseq2 package (1.4.5 version; Love et al., 2014), whereby the read count of the group B spike-in RNAs was used to calculate the DEseq2 sizeFactor, since the concentration of group B spike-in RNAs should be constant between the two spike-in mixes used across all samples. This approach ensures that the RNA-seq libraries are scaled to reference spike-in controls, and not to the sequencing depth of the library (Srivastava et al., 2018). Differentially expressed genes using both these normalization approaches were then identified for each pairwise comparison (Tables S4–S6). To assess the correlation between replicates and samples, the dissimilarity between the samples and replicates was computed using the

normalized gene count matrix to obtain sample-to-sample distances as calculated by the Euclidean Distance Method of the DESeq package (Anders and Huber, 2010). The distance matrix was further clustered hierarchically and plotted as a heat map (Fig. S2A). The Panther (version 13.1) and g:Profiler tool (g:Cocoa; Reimand et al., 2011) was used for overrepresentation analysis of GO terms for single and multiple gene lists, respectively, For cross-comparison of MB and G_0 transcriptomes with published expression profiles of primary MuSCs, the expression counts for quiescent and activated MuSCs (Yue et al., 2020) were obtained from GEO accession GSE113631 (https://www.ncbi.nlm.nih.gov/geo/query/acc.cgi?acc=GSE113631). Further processing to compare datasets from different experiments (cultured myoblast data from this work versus published datasets from MuSCs) was carried out in R (https://www.r-project.org/), wherein expression data were first quantile-normalized using 'preprocessCore', followed by batch correction. PCA plot generation was performed using the 'BatchQC' Shiny App package (Manimaran et al., 2016).

qPCR validation of RNA-seq data

Equal numbers of MBs and G_0 cells were harvested, and triplicate samples were counted using Trypan Blue exclusion to generate a live-cell count in a Countess Automated Cell Counter (Invitrogen). Cells were lysed using 350 µl RLT buffer (RNeasy Micro Kit, Qiagen) containing β-mercaptoethanol, and lysates were vortexed vigorously to shear genomic DNA and then stored at −70°C until further processing. RNA was isolated using an RNeasy Micro Kit (Qiagen, 74004) as per the manufacturer's protocol, using an RNeasy MinElute spin column, and was eluted in 14 µl of nuclease-free water. RNA was quantified using a NanoDrop ND-1000UV-Vis spectrophotometer (NanoDrop Technologies). The following samples were drawn from MB and G_0 RNA for cDNA preparation: (1) MB-ER, 500 ng of MB RNA; (2) G_0-ER, 500 ng of G_0 RNA; (3) MB-EC, RNA equivalent of 73,000 MBs; (4) G_0-EC: RNA equivalent of 73,000 G_0 cells. cDNA was synthesized using the SuperScript IV First-Strand Synthesis System (Invitrogen, 18091050) by following the manufacturer's protocol. RT-qPCR was performed using SYBR Green reagent (Power SYBR Green PCR Master Mix; ABI, 4367659) with appropriate primer pairs on an ABI ViiA7 real-time PCR system. Fold change of gene expression in G_0 cells relative to MBs was calculated using the ΔCt method [$\log(Ct_{G0}-Ct_{MB})$] within the two sets: equal RNA (ER) and equal cell number (EC) (Fig. S2C).

ChIP-seq data analysis

After quality assessment, raw ChIP-seq reads were aligned to the *M. musculus* reference genome (NCBIM37/mm9) using the paired option of Bowtie2 (2.0.1; Langmead and Salzberg, 2012). To calculate RNAPII enrichment at TSSs, only non-overlapping genes of more than 2500 bp were used for analysis. Using these criteria, 15,170 genes were used for analysis. The read density counts around the TSS (±300 bp) was enumerated for all samples. Independently for each cell state (MB or G_0), the TSS regions were sub-grouped into >90th percentile and 80–90th percentile based on read density score sorted from lowest to highest value. Thus, for each cell state (both input and ChIP), the average distribution of read densities was plotted for each subgroup (Fig. 2A). For stalling index analysis, only non-overlapping genes of more than 1500 bp were used – 16,095 genes met these criteria. To calculate RNAPII stalling index, the number of ChIP-seq reads at the promoter region (−50 to +300 bp from the TSS) and gene body (+300 to +2500 bp for genes longer than 2 kb and +300 to +1500 bp for genes between 1.5 kb and 2.5 kb) of each gene was enumerated using SeqMonk (https://www.bioinformatics.babraham.ac.uk/projects/seqmonk/). This window effectively rules out contributions from polymerases involved in divergent transcription, which peaks at −250 bp (Fig. S3A,B,D). To shortlist state-specific stalled genes, stalling indices of corresponding input samples were fitted to a Gaussian distribution (Zeitlinger et al., 2007). The cut-off of the mean plus three standard deviations for input was computed and used for identifying stalled genes in RNAPII pulldown samples.

Statistical analysis

R packages were used to carry out statistical significance tests. Mann–Whitney test and Student's *t*-test were used as indicated in the figure legends. For the box plots, the horizontal bar represents the median value, and the upper and lower limits of the box represent the 75th and 25th percentiles, respectively.

Acknowledgements

We thank K. Adelman, A. Ansari, B. Burgering, D. Palakodeti and A. Seshasayee for helpful discussions; M. Mokry for input to customize the ChIP-seq analysis pipeline; D. Cornelison and J. Anderson for teaching us myofiber methods; Shahragim Tajbakhsh (Institut Pasteur, Paris, France) for providing Tg:Pax7–nGFP mice; and S. Galande for critical reading of the manuscript. We gratefully acknowledge next-generation sequencing, imaging and animal facilities at the Bangalore Life Sciences Cluster and at CCMB, Hyderabad; and an InStem collaborative science chair fellowship to Boudewijn Burgering (UMC Utrecht, Utrecht, The Netherlands) and support from University of Utrecht for exchange visits between the J.D. and Boudewijn Burgering labs.

Competing interests

The authors declare no competing or financial interests.

Author contributions

Conceptualization: H.P.G., D.S., J.D.; Methodology: H.P.G., D.S., N.V., A.A.; Software: H.P.G., G.P.; Validation: H.P.G., D.S., N.V.; Formal analysis: H.P.G., D.S., A.A., G.P., J.D.; Investigation: H.P.G., D.S., N.V., A.A.; Data curation: H.P.G.; Writing - original draft: H.P.G., J.D.; Writing - review & editing: H.P.G., D.S.; Visualization: H.P.G., D.S.; Supervision: H.P.G., J.D.; Project administration: J.D.; Funding acquisition: J.D.

Funding

This work was supported by fellowships from the Council of Scientific and Industrial Research, India (CSIR; to H.P.G. and D.S.); the Department of Biotechnology, Ministry of Science and Technology, India (to N.V. and G.P.); the Department of Atomic Energy, Government of India, and National Centre for Biological Sciences (NCBS; to A.A.); and CSIR-CCMB (to H.P.G.). We also acknowledge support from core funds to CCMB from CSIR; and grants from Department of Biotechnology, Ministry of Science and Technology, India to J.D. [Indo-Australia (BT/Indo-Aus/05/36/2010) and Indo-Denmark (BT/IN/Denmark/08/JD/2016)]. Animal work was partially supported by the National Mouse Research Resource (NaMoR) grant (BT/PR5981/MED/31/181/2012; 2013-2016) from the Department of Biotechnology, Ministry of Science and Technology, India to NCBS.

Data availability

The ChIP-seq and RNA-seq raw data from this study have been deposited at the NCBI GEO repository with the BioProject accession PRJNA343309 (http://www.ncbi.nlm.nih.gov/bioproject/343309).

Peer review history

The peer review history is available online at https://journals.biologists.com/jcs/lookup/doi/10.1242/jcs.259789.reviewer-comments.pdf.

References

Adelman, K. and Lis, J. T. (2012). Promoter-proximal pausing of RNA polymerase II: emerging roles in metazoans. *Nat. Rev. Genet.* **13**, 720-731. doi:10.1038/nrg3293

Anders, S. and Huber, W. (2010). Differential expression analysis for sequence count data. *Genome Biol.* **11**, R106. doi:10.1186/gb-2010-11-10-r106

Anders, S., Pyl, P. T. and Huber, W. (2015). HTSeq - a Python framework to work with high-throughput sequencing data. *Bioinformatics* **31**, 166-169. doi:10.1093/bioinformatics/btu638

Anderson, J. E., Wozniak, A. C. and Mizunoya, W. (2012). Single muscle-fiber isolation and culture for cellular, molecular, pharmacological, and evolutionary studies. In *Myogenesis: Methods and Protocols* (ed. J. X. DiMario), pp. 85-102. Totowa, NJ: Humana Press.

Badhai, J., Fröjmark, A.-S., Davey, E. J., Schuster, J. and Dahl, N. (2009). Ribosomal protein S19 and S24 insufficiency cause distinct cell cycle defects in Diamond-Blackfan anemia. *Biochim. Biophys. Acta* **1792**, 1036-1042. doi:10.1016/j.bbadis.2009.08.002

Benecke, B.-J., Ben-Ze'ev, A. and Penman, S. (1978). The control of mRNA production, translation and turnover in suspended and reattached anchorage-dependent fibroblasts. *Cell* **14**, 931-939. doi:10.1016/0092-8674(78)90347-1

Bertoli, C., Skotheim, J. M. and de Bruin, R. A. M. (2013). Control of cell cycle transcription during G1 and S phases. *Nat. Rev. Mol. Cell Biol.* **14**, 518-528. doi:10.1038/nrm3629

Boonsanay, V., Zhang, T., Georgieva, A., Kostin, S., Qi, H., Yuan, X., Zhou, Y. and Braun, T. (2016). Regulation of skeletal muscle stem cell quiescence by Suv4-20h1-dependent facultative heterochromatin formation. *Cell Stem Cell* **18**, 229-242. doi:10.1016/j.stem.2015.11.002

Carnac, G., Fajas, L., L'honoré, A., Sardet, C., Lamb, N. J. C. and Fernandez, A. (2000). The retinoblastoma-like protein p130 is involved in the determination of reserve cells in differentiating myoblasts. *Curr. Biol.* **10**, 543-546. doi:10.1016/S0960-9822(00)00471-1

Carpenter, A. E., Jones, T. R., Lamprecht, M. R., Clarke, C., Kang, I. H., Friman, O., Guertin, D. A., Chang, J. H., Lindquist, R. A., Moffat, J. et al. (2006). CellProfiler: image analysis software for identifying and quantifying cell phenotypes. *Genome Biol.* **7**, R100. doi:10.1186/gb-2006-7-10-r100

Cheedipudi, S., Puri, D., Saleh, A., Gala, H. P., Rumman, M., Pillai, M. S., Sreenivas, P., Arora, R., Sellathurai, J., Schrøder, H. D. et al. (2015). A fine balance: epigenetic control of cellular quiescence by the tumor suppressor PRDM2/RIZ at a bivalent domain in the cyclin a gene. *Nucleic Acids Res.* **43**, 6236-6256. doi:10.1093/nar/gkv567

Cheung, T. H. and Rando, T. A. (2013). Molecular regulation of stem cell quiescence. *Nat. Rev. Mol. Cell Biol.* **14**, 329-340. doi:10.1038/nrm3591

Cho, E.-J., Kobor, M. S., Kim, M., Greenblatt, J. and Buratowski, S. (2001). Opposing effects of Ctk1 kinase and Fcp1 phosphatase at Ser 2 of the RNA polymerase II C-terminal domain. *Genes Dev.* **15**, 3319-3329. doi:10.1101/gad.935901

Choesmel, V., Fribourg, S., Aguissa-Touré, A.-H., Pinaud, N., Legrand, P., Gazda, H. T. and Gleizes, P.-E. (2008). Mutation of ribosomal protein RPS24 in Diamond-Blackfan anemia results in a ribosome biogenesis disorder. *Hum. Mol. Genet.* **17**, 1253-1263. doi:10.1093/hmg/ddn015

Coller, H. A. (2007). What's taking so long? S-phase entry from quiescence versus proliferation. *Nat. Rev. Mol. Cell Biol.* **8**, 667-670. doi:10.1038/nrm2223

Coller, H. A., Sang, L. and Roberts, J. M. (2006). A new description of cellular quiescence. *PLoS Biol.* **4**, e83. doi:10.1371/journal.pbio.0040083

Collins, C. A., Zammit, P. S., Ruiz, A. P., Morgan, J. E. and Partridge, T. A. (2007). A population of myogenic stem cells that survives skeletal muscle aging. *Stem Cells Dayt. Ohio* **25**, 885-894. doi:10.1634/stemcells.2006-0372

Darzynkiewicz, Z., Traganos, F. and Melamed, M. R. (1980). New cell cycle compartments identified by multiparameter flow cytometry. *Cytometry* **1**, 98-108. doi:10.1002/cyto.990010203

Deato, M. D. E. and Tjian, R. (2007). Switching of the core transcription machinery during myogenesis. *Genes Dev.* **21**, 2137-2149. doi:10.1101/gad.1583407

Deng, P., Wang, J., Zhang, X., Wu, X., Ji, N., Li, J., Zhou, M., Jiang, L., Zeng, X. and Chen, Q. (2018). AFF4 promotes tumorigenesis and tumor-initiation capacity of head and neck squamous cell carcinoma cells by regulating SOX2. *Carcinogenesis* **39**, 937-947. doi:10.1093/carcin/bgy046

Doles, J. D. and Olwin, B. B. (2015). Muscle stem cells on the edge. *Curr. Opin. Genet. Dev.* **34**, 24-28. doi:10.1016/j.gde.2015.06.006

Everetts, A. G., Manning, A. L., Wang, X., Dyson, N. J., Garcia, B. A. and Coller, H. A. (2013). H4K20 methylation regulates quiescence and chromatin compaction. *Mol. Biol. Cell* **24**, 3025-3037. doi:10.1091/mbc.e12-07-0529

Freter, R., Osawa, M. and Nishikawa, S.-I. (2010). Adult stem cells exhibit global suppression of RNA polymerase II serine-2 phosphorylation. *Stem Cells Dayt. Ohio* **28**, 1571-1580. doi:10.1002/stem.476

Fuda, N. J., Buckley, M. S., Wei, W., Core, L. J., Waters, C. T., Reinberg, D. and Lis, J. T. (2012). Fcp1 Dephosphorylation of the RNA polymerase II C-terminal domain is required for efficient transcription of heat shock genes. *Mol. Cell. Biol.* **32**, 3428-3437. doi:10.1128/MCB.00247-12

Fukada, S.-I., Uezumi, A., Ikemoto, M., Masuda, S., Segawa, M., Tanimura, N., Yamamoto, H., Miyagoe-Suzuki, Y. and Takeda, S. (2007). Molecular signature of quiescent satellite cells in adult skeletal muscle. *Stem Cells* **25**, 2448-2459. doi:10.1634/stemcells.2007-0019

Gaertner, B., Johnston, J., Chen, K., Wallaschek, N., Paulson, A., Garruss, A. S., Gaudenz, K., De Kumar, B., Krumlauf, R. and Zeitlinger, J. (2012). Poised RNA polymerase II changes over developmental time and prepares genes for future expression. *Cell Rep.* **2**, 1670-1683. doi:10.1016/j.celrep.2012.11.024

Galatioto, J., Mascareno, E. and Siddiqui, M. A. Q. (2010). CLP-1 associates with MyoD and HDAC to restore skeletal muscle cell regeneration. *J. Cell Sci.* **123**, 3789-3795. doi:10.1242/jcs.073387

García-Prat, L., Martínez-Vicente, M., Perdiguero, E., Ortet, L., Rodríguez-Ubreva, J., Rebollo, E., Ruiz-Bonilla, V., Gutarra, S., Ballestar, E., Serrano, A. L. et al. (2016). Autophagy maintains stemness by preventing senescence. *Nature* **529**, 37-42. doi:10.1038/nature16187

Gilchrist, D. A., Nechaev, S., Lee, C., Ghosh, S. K. B., Collins, J. B., Li, L., Gilmour, D. S. and Adelman, K. (2008). NELF-mediated stalling of Pol II can enhance gene expression by blocking promoter-proximal nucleosome assembly. *Genes Dev.* **22**, 1921-1933. doi:10.1101/gad.1643208

Ginisty, H., Amalric, F. and Bouvet, P. (1998). Nucleolin functions in the first step of ribosomal RNA processing. *EMBO J.* **17**, 1476-1486. doi:10.1093/emboj/17.5.1476

Hannan, K. M., Kennedy, B. K., Cavanaugh, A. H., Hannan, R. D., Hirschler-Laszkiewicz, I., Jefferson, L. S. and Rothblum, L. I. (2000). RNA polymerase I transcription in confluent cells: Rb downregulates rDNA transcription during confluence-induced cell cycle arrest. *Oncogene* **19**, 3487-3497. doi:10.1038/sj.onc.1203690

Hausburg, M. A., Doles, J. D., Clement, S. L., Cadwallader, A. B., Hall, M. N., Blackshear, P. J., Lykke-Andersen, J. and Olwin, B. B. (2015). Post-transcriptional regulation of satellite cell quiescence by TTP-mediated mRNA decay. *eLife* **4**, e03390. doi:10.7554/eLife.03390

Hu, H., Zhang, Y., Zhao, L., Zhao, W., Wang, X., Ye, E., Dong, Y., Zhang, L., Ran, F., Zhou, Y. et al. (2021). AFF4 facilitates melanoma cell progression by regulating c-Jun activity. *Exp. Cell Res.* **399**, 112445. doi:10.1016/j.yexcr.2020.112445

Iyer, V. R., Eisen, M. B., Ross, D. T., Schuler, G., Moore, T., Lee, J. C. F., Trent, J. M., Staudt, L. M., Hudson, J., Boguski, M. S. et al. (1999). The transcriptional program in the response of human fibroblasts to serum. *Science* **283**, 83-87. doi:10.1126/science.283.5398.83

Jao, C. Y. and Salic, A. (2008). Exploring RNA transcription and turnover in vivo by using click chemistry. *Proc. Natl. Acad. Sci. USA* **105**, 15779-15784. doi:10.1073/pnas.0808480105

Jonkers, I. and Lis, J. T. (2015). Getting up to speed with transcription elongation by RNA polymerase II. *Nat. Rev. Mol. Cell Biol.* **16**, 167-177. doi:10.1038/nrm3953

Juan, A. H., Derfoul, A., Feng, X., Ryall, J. G., Dell'Orso, S., Pasut, A., Zare, H., Simone, J. M., Rudnicki, M. A. and Sartorelli, V. (2011). Polycomb EZH2 controls self-renewal and safeguards the transcriptional identity of skeletal muscle stem cells. *Genes Dev.* **25**, 789-794. doi:10.1101/gad.2027911

Kamentsky, L., Jones, T. R., Fraser, A., Bray, M.-A., Logan, D. J., Madden, K. L., Ljosa, V., Rueden, C., Eliceiri, K. W. and Carpenter, A. E. (2011). Improved structure, function and compatibility for CellProfiler: modular high-throughput image analysis software. *Bioinformatics* **27**, 1179-1180. doi:10.1093/bioinformatics/btr095

Kami, K., Noguchi, K. and Senba, E. (1995). Localization of myogenin, c-fos, c-jun, and muscle-specific gene mRNAs in regenerating rat skeletal muscle. *Cell Tissue Res.* **280**, 11-19. doi:10.1007/BF00304506

Katagi, H., Takata, N., Aoi, Y., Zhang, Y., Rendleman, E. J., Blyth, G. T., Eckerdt, F. D., Tomita, Y., Sasaki, T., Saratsis, A. M. et al. (2021). Therapeutic targeting of transcriptional elongation in diffuse intrinsic pontine glioma. *Neuro-Oncol.* **23**, 1348-1359. doi:10.1093/neuonc/noab009

Kobor, M. S., Archambault, J., Lester, W., Holstege, F. C. P., Gileadi, O., Jansma, D. B., Jennings, E. G., Kouyoumdjian, F., Davidson, A. R., Young, R. A. et al. (1999). An unusual eukaryotic protein phosphatase required for transcription by RNA polymerase II and CTD dephosphorylation in S. cerevisiae. *Mol. Cell* **4**, 55-62. doi:10.1016/S1097-2765(00)80187-2

Kõivomägi, M., Swaffer, M. P., Turner, J. J., Marinov, G. and Skotheim, J. M. (2021). G1 cyclin–Cdk promotes cell cycle entry through localized phosphorylation of RNA polymerase II. *Science* **374**, 347-351. doi:10.1126/science.aba5186

Kouzine, F., Wojtowicz, D., Yamane, A., Resch, W., Kieffer-Kwon, K.-R., Bandle, R., Nelson, S., Nakahashi, H., Awasthi, P., Feigenbaum, L. et al. (2013). Global regulation of promoter melting in naive lymphocytes. *Cell* **153**, 988-999. doi:10.1016/j.cell.2013.04.033

Kuehner, J. N., Pearson, E. L. and Moore, C. (2011). Unravelling the means to an end: RNA polymerase II transcription termination. *Nat. Rev. Mol. Cell Biol.* **12**, 283-294. doi:10.1038/nrm3098

Kühl, N. M. and Rensing, L. (2000). Heat shock effects on cell cycle progression. *Cell. Mol. Life Sci. CMLS* **57**, 450-463. doi:10.1007/PL00000707

Langmead, B. and Salzberg, S. L. (2012). Fast gapped-read alignment with Bowtie 2. *Nat. Methods* **9**, 357-359. doi:10.1038/nmeth.1923.

Lau, L. F. and Nathans, D. (1985). Identification of a set of genes expressed during the G0/G1 transition of cultured mouse cells. *EMBO J.* **4**, 3145-3151. doi:10.1002/j.1460-2075.1985.tb04057.x

Leiter, J. R. S. and Anderson, J. E. (2010). Satellite cells are increasingly refractory to activation by nitric oxide and stretch in aged mouse-muscle cultures. *Int. J. Biochem. Cell Biol.* **42**, 132-136. doi:10.1016/j.biocel.2009.09.021

Levine, M. (2011). Paused RNA polymerase II as a developmental checkpoint. *Cell* **145**, 502-511. doi:10.1016/j.cell.2011.04.021

Litovchick, L., Chestukhin, A. and DeCaprio, J. A. (2004). Glycogen synthase kinase 3 phosphorylates RBL2/p130 during quiescence. *Mol. Cell. Biol.* **24**, 8970-8980. doi:10.1128/MCB.24.20.8970-8980.2004

Liu, L., Cheung, T. H., Charville, G. W., Hurgo, B. M. C., Leavitt, T., Shih, J., Brunet, A. and Rando, T. A. (2013). Chromatin modifications as determinants of muscle stem cell quiescence and chronological aging. *Cell Rep.* **4**, 189-204. doi:10.1016/j.celrep.2013.05.043

Love, M .I., Huber, W. and Anders, S. (2014). Moderated estimation of fold change and dispersion for RNA-seq data with DESeq2. *Genome Biol.* **15**, 550. doi:10.1186/s13059-014-0550-8

Lovén, J., Orlando, D. A., Sigova, A. A., Lin, C. Y., Rahl, P. B., Burge, C. B., Levens, D. L., Lee, T. I. and Young, R. A. (2012). Revisiting Global Gene Expression Analysis. *Cell* **151**, 476-482. doi:10.1016/j.cell.2012.10.012

Lu, X., Zhu, X., Li, Y., Liu, M., Yu, B., Wang, Y., Rao, M., Yang, H., Zhou, K., Wang, Y. et al. (2016). Multiple P-TEFbs cooperatively regulate the release of promoter-proximally paused RNA polymerase II. *Nucleic Acids Res.* **44**, 6853-6867. doi:10.1093/nar/gkw571

Luo, Z., Lin, C., Guest, E., Garrett, A. S., Mohaghegh, N., Swanson, S., Marshall, S., Florens, L., Washburn, M. P. and Shilatifard, A. (2012). The super

elongation complex family of RNA polymerase II elongation factors: gene target specificity and transcriptional output. *Mol. Cell. Biol.* **32**, 2608-2617. doi:10.1128/MCB.00182-12

Machado, L., de Lima, J. E., Fabre, O., Proux, C., Legendre, R., Szegedi, A., Varet, H., Ingerslev, L. R., Barrès, R., Relaix, F. et al. (2017). In situ fixation redefines quiescence and early activation of skeletal muscle stem cells. *Cell Rep.* **21**, 1982-1993. doi:10.1016/j.celrep.2017.10.080

Malecova, B., Dall'Agnese, A., Madaro, L., Gatto, S., Toto, P. C., Albini, S., Ryan, T., Tora, L. and Puri, P. L. (2016). TBP/TFIID-dependent activation of MyoD target genes in skeletal muscle cells. *eLife* **5**, e12534. doi:10.7554/eLife.12534

Mandal, S. S., Cho, H., Kim, S., Cabane, K. and Reinberg, D. (2002). FCP1, a phosphatase specific for the heptapeptide repeat of the largest subunit of RNA polymerase II, stimulates transcription elongation. *Mol. Cell. Biol.* **22**, 7543-7552. doi:10.1128/MCB.22.21.7543-7552.2002

Manimaran, S., Selby, H. M., Okrah, K., Ruberman, C., Leek, J. T., Quackenbush, J., Haibe-Kains, B., Bravo, H. C. and Johnson, W. E. (2016). BatchQC: interactive software for evaluating sample and batch effects in genomic data. *Bioinformatics* **32**, 3836-3838. doi:10.1093/bioinformatics/btw538

Margaritis, T. and Holstege, F. C. P. (2008). Poised RNA polymerase II gives pause for thought. *Cell* **133**, 581-584. doi:10.1016/j.cell.2008.04.027

Maxwell, C. S., Kruesi, W. S., Core, L. J., Kurhanewicz, N., Waters, C. T., Lewarch, C. L., Antoshechkin, I., Lis, J. T., Meyer, B. J. and Baugh, L. R. (2014). Pol II docking and pausing at growth and stress genes in C. elegans. *Cell Rep.* **6**, 455-466. doi:10.1016/j.celrep.2014.01.008

Milasincic, D. J., Dhawan, J. and Farmer, S. R. (1996). Anchorage-dependent control of muscle-specific gene expression in C2C12 mouse myoblasts. *Vitro Cell. Dev. Biol. Anim.* **32**, 90-99. doi:10.1007/BF02723040

Mousavi, K., Zare, H., Wang, A. H. and Sartorelli, V. (2012). Polycomb protein Ezh1 promotes RNA polymerase II elongation. *Mol. Cell* **45**, 255-262. doi:10.1016/j.molcel.2011.11.019

Nakajima, T., Inui, S., Fushimi, T., Noguchi, F., Kitagawa, Y., Reddy, J. K. and Itami, S. (2013). Roles of MED1 in quiescence of hair follicle stem cells and maintenance of normal hair cycling. *J. Invest. Dermatol.* **133**, 354-360. doi:10.1038/jid.2012.293

Narita, T., Yamaguchi, Y., Yano, K., Sugimoto, S., Chanarat, S., Wada, T., Kim, D.-K., Hasegawa, J., Omori, M., Inukai, N. et al. (2003). Human transcription elongation factor NELF: identification of novel subunits and reconstitution of the functionally active complex. *Mol. Cell. Biol.* **23**, 1863-1873. doi:10.1128/MCB.23.6.1863-1873.2003

Oki, T., Nishimura, K., Kitaura, J., Togami, K., Maehara, A., Izawa, K., Sakaue-Sawano, A., Niida, A., Miyano, S., Aburatani, H. et al. (2014). A novel cell-cycle-indicator, mVenus-p27K^{-}, identifies quiescent cells and visualizes G0–G1 transition. *Sci. Rep.* **4**, 4012. doi:10.1038/srep04012

Pallafacchina, G., François, S., Regnault, B., Czarny, B., Dive, V., Cumano, A., Montarras, D. and Buckingham, M. (2010). An adult tissue-specific stem cell in its niche: A gene profiling analysis of in vivo quiescent and activated muscle satellite cells. *Stem Cell Res.* **4**, 77-91. doi:10.1016/j.scr.2009.10.003

Pledger, W. J., Stiles, C. D., Antoniades, H. N. and Scher, C. D. (1978). An ordered sequence of events is required before BALB/c-3T3 cells become committed to DNA synthesis. *Proc. Natl. Acad. Sci. USA* **75**, 2839-2843. doi:10.1073/pnas.75.6.2839

Puri, D., Gala, H., Mishra, R. and Dhawan, J. (2015). High-wire act: the poised genome and cellular memory. *FEBS J.* **282**, 1675-1691. doi:10.1111/febs.13165

Radonjic, M., Andrau, J.-C., Lijnzaad, P., Kemmeren, P., Kockelkorn, T. T. J. P., van Leenen, D., van Berkum, N. L. and Holstege, F. C. P. (2005). Genome-wide analyses reveal RNA polymerase II located upstream of genes poised for rapid response upon S. cerevisiae stationary phase exit. *Mol. Cell* **18**, 171-183. doi:10.1016/j.molcel.2005.03.010

Reimand, J., Arak, T. and Vilo, J. (2011). g:Profiler - a web server for functional interpretation of gene lists (2011 update). *Nucleic Acids Res.* **39**, W307-W315. doi:10.1093/nar/gkr378

Robinson, D. C. L., Ritso, M., Nelson, G. M., Mokhtari, Z., Nakka, K., Bandukwala, H., Goldman, S. R., Park, P. J., Mounier, R., Chazaud, B. et al. (2021). Negative elongation factor regulates muscle progenitor expansion for efficient myofiber repair and stem cell pool repopulation. *Dev. Cell* **56**, 1014-1029.e7. doi:10.1016/j.devcel.2021.02.025

Rodgers, J. T., King, K. Y., Brett, J. O., Cromie, M. J., Charville, G. W., Maguire, K. K., Brunson, C., Mastey, N., Liu, L., Tsai, C.-R. et al. (2014). mTORC1 controls the adaptive transition of quiescent stem cells from G0 to G(Alert). *Nature* **510**, 393-396. doi:10.1038/nature13255

Roy, N., Sundar, S., Pillai, M., Patell-Socha, F., Ganesh, S., Aloysius, A., Rumman, M., Gala, H., Hughes, S. M., Zammit, P. S. et al. (2021). mRNP granule proteins Fmrp and Dcp1a differentially regulate mRNP complexes to contribute to control of muscle stem cell quiescence and activation. *Skelet. Muscle* **11**, 18. doi:10.1186/s13395-021-00270-9

Rumman, M., Majumder, A., Harkness, L., Venugopal, B., Vinay, M. B., Pillai, M. S., Kassem, M. and Dhawan, J. (2018). Induction of quiescence (G0) in bone marrow stromal stem cells enhances their stem cell characteristics. *Stem Cell Res.* **30**, 69-80. doi:10.1016/j.scr.2018.05.010

Russell, J. and Zomerdijk, J. C. B. M. (2005). RNA-polymerase-I-directed rDNA transcription, life and works. *Trends Biochem. Sci.* **30**, 87-96. doi:10.1016/j.tibs.2004.12.008

Sachidanandan, C., Sambasivan, R. and Dhawan, J. (2002). Tristetraprolin and LPS-inducible CXC chemokine are rapidly induced in presumptive satellite cells in response to skeletal muscle injury. *J. Cell Sci.* **115**, 2701-2712. doi:10.1242/jcs.115.13.2701

Saha, R. N., Wissink, E. M., Bailey, E. R., Zhao, M., Fargo, D. C., Hwang, J., Daigle, K. R., Fenn, J. D., Adelman, K. and Dudek, S. M. (2011). Rapid activity-induced transcription of arc and other IEGs relies on poised RNA polymerase II. *Nat. Neurosci.* **14**, 848-856. doi:10.1038/nn.2839

Sajiki, K., Hatanaka, M., Nakamura, T., Takeda, K., Shimanuki, M., Yoshida, T., Hanyu, Y., Hayashi, T., Nakaseko, Y. and Yanagida, M. (2009). Genetic control of cellular quiescence in S. pombe. *J. Cell Sci.* **122**, 1418-1429. doi:10.1242/jcs.046466

Sambasivan, R., Gayraud-Morel, B., Dumas, G., Cimper, C., Paisant, S., Kelly, R. G., Kelly, R. and Tajbakhsh, S. (2009). Distinct regulatory cascades govern extraocular and pharyngeal arch muscle progenitor cell fates. *Dev. Cell* **16**, 810-821. doi:10.1016/j.devcel.2009.05.008

Scheidegger, A. and Nechaev, S. (2016). RNA Polymerase II Pausing as a Context-Dependent Reader of the Genome. *Biochem. Cell Biol. Biochim. Biol. Cell.* **94**, 82-92. doi:10.1139/bcb-2015-0045

Schnerch, D., Yalcintepe, J., Schmidts, A., Becker, H., Follo, M., Engelhardt, M. and Wäsch, R. (2012). Cell cycle control in acute myeloid leukemia. *Am. J. Cancer Res.* **2**, 508-528.

Scott, P. H., Cairns, C. A., Sutcliffe, J. E., Alzuherri, H. M., McLees, A., Winter, A. G. and White, R. J. (2001). Regulation of RNA polymerase III transcription during cell cycle entry. *J. Biol. Chem.* **276**, 1005-1014. doi:10.1074/jbc.M005417200

Sebastian, S., Sreenivas, P., Sambasivan, R., Cheedipudi, S., Kandalla, P., Pavlath, G. K. and Dhawan, J. (2009). MLL5, a trithorax homolog, indirectly regulates H3K4 methylation, represses cyclin A2 expression, and promotes myogenic differentiation. *Proc. Natl. Acad. Sci. USA* **106**, 4719-4724. doi:10.1073/pnas.0807136106

Shefer, G. and Yablonka-Reuveni, Z. (2005). Isolation and culture of skeletal muscle myofibers as a means to analyze satellite cells. *Methods Mol. Biol.* **290**, 281-304. doi:10.1385/1-59259-838-2:281

Siegel, A. L., Atchison, K., Fisher, K. E., Davis, G. E. and Cornelison, D. D. W. (2009). 3D timelapse analysis of muscle satellite cell motility. *Stem Cells Dayt.* **27**, 2527-2538. doi:10.1002/stem.178

Song, B., Zhang, Q., Zhang, Z., Wan, Y., Jia, Q., Wang, X., Zhu, X., Leung, A. Y.-H., Cheng, T., Fang, X. et al. (2014). Systematic transcriptome analysis of the zebrafish model of diamond-blackfan anemia induced by RPS24 deficiency. *BMC Genomics* **15**, 759. doi:10.1186/1471-2164-15-759

Sousa-Victor, P., Gutarra, S., García-Prat, L., Rodriguez-Ubreva, J., Ortet, L., Ruiz-Bonilla, V., Jardí, M., Ballestar, E., González, S., Serrano, A. L. et al. (2014). Geriatric muscle stem cells switch reversible quiescence into senescence. *Nature* **506**, 316-321. doi:10.1038/nature13013

Srivastava, S., Mishra, R. K. and Dhawan, J. (2010). Regulation of cellular chromatin state: insights from quiescence and differentiation. *Organogenesis* **6**, 37-47. doi:10.4161/org.6.1.11337

Srivastava, S., Gala, H. P., Mishra, R. K. and Dhawan, J. (2018). Distinguishing states of arrest: genome-wide descriptions of cellular quiescence using ChIP-seq and RNA-seq analysis. *Methods Mol. Biol.* **1686**, 215-239. doi:10.1007/978-1-4939-7371-2_16

Subramaniam, S., Sreenivas, P., Cheedipudi, S., Reddy, V. R., Shashidhara, L. S., Chilukoti, R. K., Mylavarapu, M. and Dhawan, J. (2013). Distinct transcriptional networks in quiescent myoblasts: a role for Wnt signaling in reversible vs. irreversible arrest. *PLoS ONE* **8**, e65097. doi:10.1371/journal.pone.0065097

Trapnell, C., Roberts, A., Goff, L., Pertea, G., Kim, D., Kelley, D. R., Pimentel, H., Salzberg, S. L., Rinn, J. L. and Pachter, L. (2012). Differential gene and transcript expression analysis of RNA-seq experiments with TopHat and Cufflinks. *Nat. Protoc.* **7**, 562-578. doi:10.1038/nprot.2012.016

Ugrinova, I., Monier, K., Ivaldi, C., Thiry, M., Storck, S., Mongelard, F. and Bouvet, P. (2007). Inactivation of nucleolin leads to nucleolar disruption, cell cycle arrest and defects in centrosome duplication. *BMC Mol. Biol.* **8**, 66. doi:10.1186/1471-2199-8-66

van Velthoven, C. T. J., de Morree, A., Egner, I. M., Brett, J. O. and Rando, T. A. (2017). Transcriptional profiling of quiescent muscle stem cells in vivo. *Cell Rep.* **21**, 1994-2004. doi:10.1016/j.celrep.2017.10.037

Venezia, T. A., Merchant, A. A., Ramos, C. A., Whitehouse, N. L., Young, A. S., Shaw, C. A. and Goodell, M. A. (2004). Molecular signatures of proliferation and quiescence in hematopoietic stem cells. *PLoS Biol.* **2**, e301. doi:10.1371/journal.pbio.0020301

White, R. J., Gottlieb, T. M., Downes, C. S. and Jackson, S. P. (1995). Cell cycle regulation of RNA polymerase III transcription. *Mol. Cell. Biol.* **15**, 6653-6662. doi:10.1128/MCB.15.12.6653

Williams, L. H., Fromm, G., Gokey, N. G., Henriques, T., Muse, G. W., Burkholder, A., Fargo, D. C., Hu, G. and Adelman, K. (2015). Pausing of

RNA polymerase II regulates mammalian developmental potential through control of signaling networks. *Mol. Cell* **58**, 311-322. doi:10.1016/j.molcel.2015.02.003

Woodhouse, S., Pugazhendhi, D., Brien, P. and Pell, J. M. (2013). Ezh2 maintains a key phase of muscle satellite cell expansion but does not regulate terminal differentiation. *J. Cell Sci.* **126**, 565-579. doi:10.1242/jcs.114843

Wu, F., Nie, S., Yao, Y., Huo, T., Li, X., Wu, X., Zhao, J., Lin, Y.-L., Zhang, Y., Mo, Q. et al. (2021). Small-molecule inhibitor of AF9/ENL-DOT1L/AF4/AFF4 interactions suppresses malignant gene expression and tumor growth. *Theranostics* **11**, 8172-8184. doi:10.7150/thno.56737

Yamaguchi, Y., Takagi, T., Wada, T., Yano, K., Furuya, A., Sugimoto, S., Hasegawa, J. and Handa, H. (1999). NELF, a multisubunit complex containing RD, cooperates with DSIF to repress RNA polymerase II elongation. *Cell* **97**, 41-51. doi:10.1016/S0092-8674(00)80713-8

Yonaha, M., Chibazakura, T., Kitajima, S. and Yasukochi, Y. (1995). Cell cycle-dependent regulation of RNA polymerase II basal transcription activity. *Nucleic Acids Res.* **23**, 4050-4054. doi:10.1093/nar/23.20.4050

Yoshida, N., Yoshida, S., Koishi, K., Masuda, K. and Nabeshima, Y. (1998). Cell heterogeneity upon myogenic differentiation: down-regulation of MyoD and Myf-5 generates “reserve cells”. *J. Cell Sci.* **111**, 769-779. doi:10.1242/jcs.111.6.769

Yue, L., Wan, R., Luan, S., Zeng, W. and Cheung, T. H. (2020). Dek modulates global intron retention during muscle stem cells quiescence exit. *Dev. Cell* **53**, 661-676.e6. doi:10.1016/j.devcel.2020.05.006

Zeitlinger, J., Stark, A., Kellis, M., Hong, J.-W., Nechaev, S., Adelman, K., Levine, M. and Young, R. A. (2007). RNA polymerase stalling at developmental control genes in the Drosophila melanogaster embryo. *Nat. Genet.* **39**, 1512-1516. doi:10.1038/ng.2007.26

Zhang, H. and Anderson, J. E. (2014). Satellite cell activation and populations on single muscle-fiber cultures from adult zebrafish (Danio rerio). *J. Exp. Biol.* **217**, 1910-1917. doi:10.1242/jeb.102210

Zhang, D. W., Rodríguez-Molina, J. B., Tietjen, J. R., Nemec, C. M. and Ansari, A. Z. (2012). Emerging views on the CTD code. *Genet. Res. Int.* **2012**, 347214. doi:10.1155/2012/347214

Zhong, R., Ge, X., Chu, T., Teng, J., Yan, B., Pei, J., Jiang, L., Zhong, H. and Han, B. (2016). Lentivirus-mediated knockdown of CTDP1 inhibits lung cancer cell growth in vitro. *J. Cancer Res. Clin. Oncol.* **142**, 723-732. doi:10.1007/s00432-015-2070-7

Zhou, C., Xiong, Q., Zhu, X., Du, W., Deng, P., Li, X., Jiang, Y., Zou, S., Wang, C. and Yuan, Q. (2017). AFF1 and AFF4 differentially regulate the osteogenic differentiation of human MSCs. *Bone Res.* **5**, 1-10. doi:10.1038/boneres.2017.44